Chapter 17

Scale up of chemical reactors

Gianni Donati *, Renato Paludetto

Research Department Snamprogetti S.p.A., Via Maritano, 26, 20097 S. Donato Milanese, Italy
Enichem S.p.A., Istituto Guido Donegani, Via Fauser, 50, 28100 Novara, Italy

1. Scale up and process innovation

Even if often no distinction is made between invention and innovation, the difference is definitely not a subtle one.

As a matter of fact, it is not always possible to turn a good idea into an innovation and put it into practice: an invention can sometimes lay unused for ages without paying back in terms of industrial realization and of profitable business.

This review will not go into discussion on issue related to the market, nor will deal with the attitude of companies and management to promote innovation. We shall focus instead on the technical knowledge and on the tools that are necessary to change an invention into a true innovation

The chemical business being mature, the attention should be paid more to the innovation of processes than to the invention of new products.

From this point of view, the study and the development of new reactors, that are able to convert raw material into products with high conversion and selectivity, play an important role in the innovation of the chemical business.

1.1. Main problems in the scaling up of reactors

Scaling up of reactors is a major task for chemical engineers and is the fundamental step in the realization and optimization of industrial plants.

The scale up activity represents the synthesis of the know how accumulated in the various phases of process development from the design of laboratory experiments and the derivation of kinetic correlations, to fluid dynamic experiments, mathematical modeling, design and operation of pilot and industrial plants.

The term "scale up" has been usually explained as "how to design a pilot or industrial reactor able to replicate through a standard methodology the results obtained in the laboratory".

This is a limiting definition, since experience has shown that it does not really exist a standard way through process innovation: actual production processes are the result of successful decisions, and sometimes of many mistakes.

---

* Corresponding author.

Crucial factors in the "scale up" are not only the technical understanding but also the ability of assuming the risk of the business.

As a matter of fact, in the past, decisions have not always been sufficiently supported by adequate experimental evidences and, even today, industrial plant operation is mainly based on experience. From the above remarks, it can be drawn a broader definition of "scale-up", as a mixture of know how, innovative ideas, standard methodologies and basic criteria with a glimmer of entrepreneurship.

With reference to chemical reactors, as the core of a process, there is no general rule and no straightforward procedure to achieve these objectives.

The reasons are many:

- kinetic data are peculiar to the reactive system. Often kinetics are masked by transport phenomena and fluid dynamics to the point that sometimes they have no relevance for the process.
- industrial scale technologies are seldom related to laboratory equipment even if industry is full of enlarged laboratory equipment.
- completely different apparatuses are possible for the same reaction and reactions can be carried out in different phases: solution, suspension, fixed beds, trickle beds, fluidized beds, distillation and extraction columns.
- other issues, often ignored in the development work, such as impurities, aging of catalysts, corrosion, fouling, safety and environmental aspects can represent a major risk for the success.

1.2. Scale up and process development

Though not an easy task, we will try to outline some basic criteria simple and general enough to act as a guide in facing the chemical reactors scale up problem. These criteria are reported in the literature but are often hidden underneath heavy mathematical approaches.

A discussion of some examples resulting from experience in the development of several processes will help in illustrating how scale up is indeed a compromise between general rules and more complex approaches.

1.2.1. Laboratory experiments

The laboratory reactor should not necessarily be similar to the idea we have of the industrial one but has to be designed in order to give the best information. In particular fluid dynamics and transport properties are to be accurately checked.

Experiments in the laboratory could follow some structural design such as the factorial or centralized ones. It is imperative, however, to investigate in a proper way the experimental space of industrial interest. Extrapolation of data and models is a risky procedure that should always be avoided.

Experiments should be carried out, if possible, in a sequential way and should be followed by a sound statistical and mathematical modeling analysis in order to improve their quality and to provide the first tools for scaling up.

Process analysis and economic evaluation, even in the first steps of research, is a sound procedure, which could even change the experimental domain of interest, improve a lot the quality of the work and help in moving fast toward the final goal.

1.2.2. Pilot scale experiments

The pilot plant is usually a costly apparatus and therefore the decision of building it is always a hard one.

A pilot plant is not intended only to prove that an existing laboratory unit yields the same results on a larger scale.

Its main purpose is to test the technologies that will be used on an industrial scale, which need not to be the same ones employed in the laboratory, in order to point out those phenomena not present on the laboratory-scale.

A pilot plant is also important to evaluate product specifications and to set up automation and control systems that will be ready for the industrial plant.

However some information on technologies do not need a real pilot. Less costly and more practical mock-up experiments made on pilot and even on larger scale cold models can help in evaluating stirring efficiencies, heat exchange, flow patterns and flow distribution, residence times, diffusion effects, etc.

The use of mock-ups followed by a clear mathematical interpretation is pushed by many factors: the incomplete knowledge available to chemical engineers on complex transport phenomena and on their scale up rules, the impossibility and the cost of building too large pilots, the difficulty of making specific measurements directly on the pilot with the real fluids and operating conditions.

Sometimes the pilot may not be strictly necessary, as for example in the case where there is an already operating industrial plant. We want however to emphasize the fact that the scope of the pilot is to be clearly stated in terms of results and quality of results expected.

In addition, following the objective, the pilot could be similar to an industrial plant or only to a part of it that needs additional investigation and demonstration.

1.2.3. Industrial unit

The operation of industrial plants has been discussed previously. The reason why plants are not so well known lays in the development and design phases and in the lack of a continuous updating of technology which is the only way to maintain competitiveness.

One formidable tool that is now available is represented by computers and automation that allow to collect data in real time, the on-line use of mathematical models and, as a consequence, a better understanding, control and optimization of plant operation.

In order to take advantage of this opportunity, all the development/scale up tests have to be performed in a more knowledge oriented and rigorous way.

The future is going to change the professional background of chemists and chemical engineers in this direction and the present requires technicians with a wide range of expertise and an open minded attitude.

Investment in new plants will probably decline in the developed countries, with increasing export of known technologies to the newly industrialized regions. There is however a lot to do on existing technology to maintain competitiveness and to stay in the chemical business.

1.2.4. Reactor technologies

This topic will be better shown in the examples. We want only to point out the key issues that are relevant in process development and are to be considered in modeling reactors.

As for catalytic gas phase reactors, critical factors that affect the selection, the modeling and design are heat exchange, effectiveness factor and aging of catalyst, flow pattern and pressure drop.

Heat exchange can be obtained with multitubular reactors, adiabatic intercooled layers or fluidized beds.

Diffusion in catalyst pores is related to rate of reaction and pellet size and is always a factor to be taken into account.

Flow pattern affects directly the yield and is managed through proper reactor design and operating conditions as a trade-off with pressure drop.

Aging or poisoning of the catalyst affects life and economy of changes and sometimes makes the process unfeasible.

Scale up of fixed bed reactors is a relatively easy task.

The fluidized bed reactor is an elegant answer to many of the problems of fixed bed and sometimes the only possible choice. The scale up is not so well known and the application has been in the past limited to those cases that had no alternative, where the advantages were relevant compared to the risk to be taken.

For homogeneous catalytic reactors the only recommendation is related to flow pattern and mixing.

Flow pattern may affect yield, selectivity and product quality and can be imposed by the reactor technology such as multitubular, vessel or cascades of stirred autoclaves.

Macro and micro mixing is important when reaction rate is competitive with these phenomena.

Gas-liquid reactors, with homogeneous or heterogeneous catalysis, in spite of the complexity of phenomena involved, have almost only one scale up variable: the interphase area per unit volume.

If the reaction rate is sufficiently high, as always is for cases of industrial interest, it occurs in a very thin layer around bubbles. Technologies that provide high interphase area are favorite and should be selected for scale up and for industrial application.

Techniques for the evaluation of bubble surface at various scales are available and are the basic tools for scaling up.

When a reaction is strongly influenced by thermodynamic equilibrium and the need of a high conversion is a valuable competitive advantage, one can combine separation technologies with reaction, which could allow to remove the products and shift equilibrium.

Example are distillation columns with reaction, reactive liquid-liquid extraction, membrane reactors.

These observations are introductory ones and need to be quantified. Before proceeding any further we need however some insight in mathematical modeling of phenomena.

2. Scale up and modeling

Scale up is the ability of finding out the quantitative rules that describe the operation of a chemical reactor at different scales, operating conditions and with different reaction technologies.

Therefore it does not only imply the capability of designing and operating large plants but also the skill of developing new and more efficient reaction technologies in order to become cost and product quality competitive and to meet environmental aspects.

Fig. 1 represents the key elements to be considered in performing this job. Not all the tools are in principle to be always taken into account and often the selection is forced by the availability of information and systems.

The procedure does not always start from laboratory to industrial but may follow an opposite path, from industrial to laboratory or it is possible to operate in parallel depending on the specific problem and the objective.

There are however three elements that should always be kept in mind and that are sometimes forgotten in industrial practice: ideas, mathematical modeling and fluid dynamic studies.

Innovative ideas are the key to the success of an industrial venture and the guideline for every R & D project.
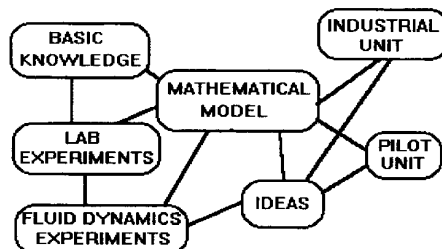
CHEMICAL ENGINEERING AND MODELLING

Fig. 1. Key elements in developing reaction technologies.

The mathematical model is the synthesis of ideas and experimental data and is the main tool to be used for scaling up or improving the performance of an industrial unit.

The mathematical model may be a simple or a complex one within available data, knowledge, ideas and objectives.

One can choose within transport phenomena models, population balance models, empirical models or combinations of them.

Examples of transport phenomena models are mass, momentum and energy balances. Population balances are based on residence time distributions. Polynomials used to fit empirical data are examples of empirical models.

We suggest to rely as much as possible on phenomenological balance equations, writing them down with the necessary complexity of description and solving them by straightforward procedures as shown by Donati et al. [21]: such models can usually be extrapolated at a certain extent beyond the experimental range of operating variables studied, while an empirical model can never be extrapolated.

Moreover, it must be always remembered the fact that, if a model gives a good description of reality, it does not necessarily mean that the assumptions upon which it is based are true.

Significant limitations are however to be recognized and formidable obstacles hinder the engineering progress.

Shortage and inaccuracy of data and the effort to estimate model parameters on the basis of experimental data is almost always the major and time consuming task.

One area of considerable importance to reaction engineering is kinetics and this is the area of greatest uncertainty. We do not need to know the "true kinetics" but we must know for sure the relation between what is derived from laboratory experiments and what is used to design an industrial reactor, side effects included. We must be able to recognize the competitive effects of kinetics and fluid dynamics: inter and intra phases transport phenomena, mixing, dead spaces and bypasses that can alter completely the performance of a reactor when compared to the "ideal" representation. These phenomena can sometime be taken into account by a theoretical approach but often require mock up experiments to be quantitatively defined. On the other hand the presence of these "defects" in the operation of "real" reactors offers an important key for scaling up and for improving the performance of industrial plants.

It is also important to understand if a further complication of the model is useful to obtain more accurate results, or if it cannot add new knowledge to scale-up.

These remarks give an hint of the difficulty in the actual use of mathematical models when applied

to scale up and analysis of a commercial plant and of the challenge that the skilled chemical engineer faces when comparing these problems.

Another possible difficulty is the availability of tools for the mathematical manipulation of equations.

This is no more a difficulty today, given the long list of computer programs available in the literature and on the market that fulfill almost every computation requirement [7,21,22,25,29]. The real problem is the availability of skilled engineers able to use these tools for their daily activity.

We have shown in an old paper [21] how even complex problems can be reduced to the solution of mass and energy balances and how equations can be written and solved with a general computerized methodology.

Other papers show [6,13,20] how experiments can be designed, kinetic data analyzed and used for the calculation of reactors.

Our effort now is focused on the topic of demonstrating how simple things can be when guided by sound ideas and by the knowledge of what can be done and of what represents a trap or a mere speculation without industrial interest.

The general cases related to different reaction technologies are intended to evidence, with a non conventional approach, the complexities and to point out a way to overcome difficulties. The applications to problems of industrial interest will show the practical way used and the results obtained.

2.1. Mathematical modeling

The application of computers to the analysis of chemical processes has been accepted as a basic tool for scaling up. Despite of this fact the discussion on this topic is still up in the air among academic people and often misunderstood in industry. During the plenary discussion in ISCRE 12 (International Symposium on Chemical Reaction Engineering, Torino, 22 June–1 July 1992) [33] the topic raised a lot of criticism.

We want to state that, apart from the different professional attitudes and tasks, a common basis of all chemical engineers is the computation and the application of matter and energy conservation principles, which is the framework of mathematical modeling.

In the already mentioned paper on this topic (Donati et al. [21]) we have shown how even complex reactors and flowsheets can be tackled in a very simple and straightforward way.

Examples of balances are the following:

2.1.1. Ideal plug flow reactors (Fig. 2)

$$\frac{dX}{d\tau} = \mathscr{R}(X,T,P)$$

$$\rho c_p \frac{dT}{d\tau} = \mathscr{R}(X,T,P)\Delta H_R + US\Delta T \tag{2.1}$$
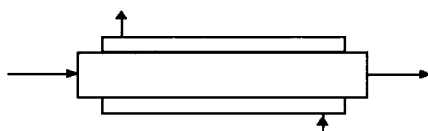

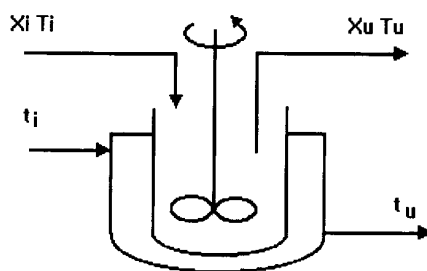Fig. 2. Scheme of the ideal plug flow reactor with jacketed countercurrent heat transfer fluid.

Fig. 3. Scheme of the continuous stirred tank with jacketed heat transfer fluid.

2.1.2. Continuous stirred tanks (Fig. 3)

$$X_u - X_i = \tau \mathscr{R}(X_u, T_u, P)$$

$$\rho\, c_p(T_u - T_i) = \tau \mathscr{R}(X_u, T_u, P)\Delta H_R + \tau\, US\Delta T \tag{2.2}$$

2.1.3. Cascades of CSTR (Fig. 4)

$$X_{u_j} - X_{i_j} = \tau \mathscr{R}\left(X_{u_j}, T_{u_j}, P\right)$$

$$\rho\, c_p\left(T_{u_j} - T_{i_j}\right) = \tau_j \mathscr{R}\left(X_{u_j}, T_{u_j}, P\right)\Delta H_R + \tau_j U_j S_j \Delta T_j \tag{2.3}$$

2.1.4. Reactors with complex fluid dynamics (isothermal) (Fig. 5)

Mass balance equations

Volume 1:

$$Q_1^F X_{j,1}^F + Q_{3,1} X_{j,3} - Q_{1,2} X_{j,1} + \mathscr{R}_{j,1} V_1 = 0 \tag{2.4}$$

Volume i:

$$Q_i^F X_{j,i}^F + Q_{1-2,i} X_{j,i-2} + Q_{i+1,i} X_{j,i+1} - Q_{i,i+2} X_{j,i} - Q_{i,i+1} X_{j,i} + \mathscr{R}_{j,i} V_i = 0$$

Volume n:

$$Q_{n-2,n} X_{j,n-2} + Q_{n,n-1} X_{j,n} - Q_n x_{j,n} + \mathscr{R}_{j,n} V_n = 0$$

Where x is a concentration (mol/m³), $\mathscr{R}$ is the reaction rate (mol/m³ s), and τ is the residence time (s) as the ratio of volume V to volumetric flowrate Q.

T, ρ, $c_p, \Delta H$ U and S are temperature, density, specific heat, reaction heat, heat exchange coefficient and heat exchange surface per unit volume.

The simpler differential equations can be solved numerically by application of the Euler or Runge Kutta integration procedures. More complex is the case of non isothermal reactors with counter current heat exchange or in the presence of important longitudinal dispersion phenomena.

Simple and complex models can however be transformed in a series of elements or "unit cells"
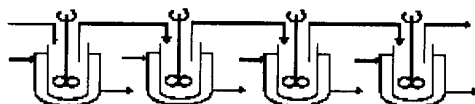

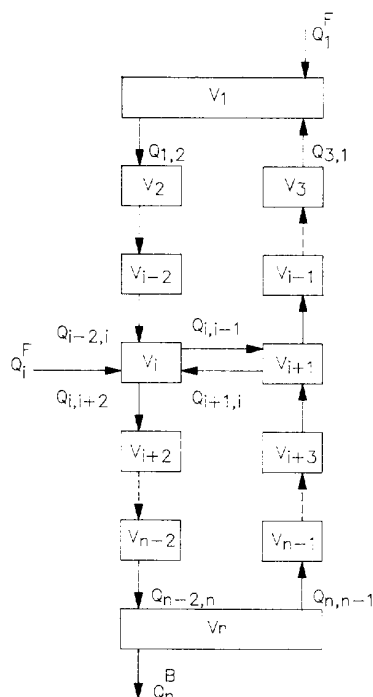Fig. 4. Scheme of CSTR cascade with jacketed heat transfer fluid.

Fig. 5. Notation for a reactor modeled as a series of unit cells.

and solved with the use of algorithms and computer programs for the solution of sparse systems of non-linear equations [21].

The approach is general and independent of the complexity, number of equations and boundary conditions.

It can be applied to modeling of local transport phenomena, to the calculation of unit operations and reactors and to the solution of mass and energy balance equation in a chemical process. The solution of equations, no matter their number nor their complexity, is up to computers, whereas the task of the engineer is essentially that of analyzing the specific problem of identifying the key issues and of formulating the balance equations at the desired level of detail.

This leads on one side to the banalization of the modeling activity and on the other side to a tremendous increase in engineering productivity, as the time wasted in trying to find out a solution can be more profitably dedicated to the creative aspects of analyzing phenomena and thinking to the relevant problems encountered in the scale up and process development activity. We again refer to the mentioned paper [21] for the details of the algorithms and procedures. The application of these simple ideas will be clear in the examples.

2.2. Fluid dynamic models

From the previous paragraph it may appear that with good ideas, experience, some knowledge of chemical engineering and a computer one can solve every problem of scaling up reactors and unit operations.

We regret to say that this is not always true. It is an habit of theoreticians to complicate the simple things and to oversimplify the complex ones.

There are topics in chemical engineering that are not completely known in terms of sound theory and where a more practical approach can easily give the desired results avoiding complex and sometimes useless mathematical computations.

Let us have for example a tank with a stirrer and baffles and assume that macro and micro mixing is important for the reaction under study.

We want to evaluate velocity patterns, how these patterns change from the small scale to the large one and possibly how to change shapes and size of stirrer and baffles, rotating speed and, maybe, to introduce other types of internals to improve reaction efficiency of the system.

We have various alternatives in how to face this problem.

The most simple models give some correlations in terms of non-dimensional numbers.

$$N_p = \frac{P}{\rho N^3 D^5} \tag{2.5}$$

$$N_q = \frac{Q}{ND^3} \tag{2.6}$$

Where N and D are the rotational speed and diameter of impeller and ρ the fluid density.

Figures for the power number N_p and discharge rate number N_q are available in the literature [43,39,15,47] for the more commonly used impellers rotating in infinite media. The geometry of tank, the presence of baffles or other internals such as heating or cooling coils and draft tube can modify significantly power input and discharge rate speed and correlations in terms of non-dimensional numbers are available for simple geometry in function of Reynolds and Froude number.

$$\left(\frac{P}{\rho N^3 D^5} \right) = \Phi[Re, Fr] \tag{2.7}$$

$$Re = \frac{D^2 N \rho}{\mu} \tag{2.8}$$

$$Fr = \frac{DN^2}{g} \tag{2.9}$$

(See Fig. 6).

These however give only a rough idea on mixing that may not suffice for chemical reactors characterization and scale up.

The more detailed approach of integrating Navier–Stokes equations cannot be easily practiced because of heavy calculations involved even for simple geometry. In spite the big effort dedicated in the last decade to computational fluid dynamics, the effect of impeller shape is hard to be taken into account and complex and important phenomena such as bubble or drop distribution in multiphase reactors are outside the possibility of computation. Turbulence modeling is still today a matter of scientific investigation.

Therefore we suggest to use the simple non-dimensional number approach for deriving scale up rules of thumb and, for more precise investigations, to build mock ups. These are tanks or tubes filled with model fluids on which one can easily measure velocity profiles, residence time distribution, liquid–liquid or gas–liquid distribution and interphase area with simple experiments.
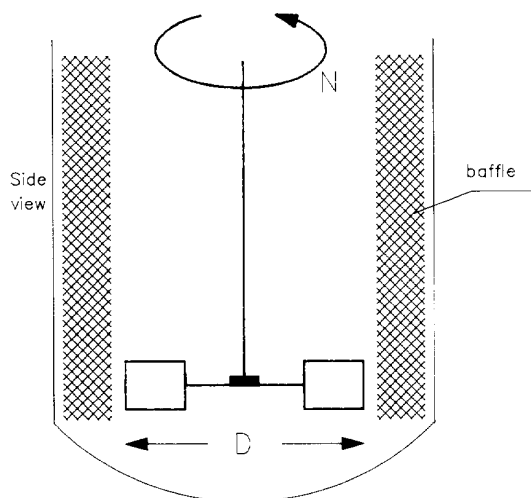
Fig. 6. Agitated tank with a six-bladed impeller and four vertical baffles.

Pitot tubes, anemometers, capacitors, conductimeters and even model fluids and reactions can be used for the scope.

Wax in water can for example be utilized for studying liquid–liquid suspensions and the sulfite oxidation reaction is a sufficiently simple and known method to characterize gas–liquid interphase area.

The procedure is shown in the examples.

3. Gas phase heterogeneous reactors

Catalytic gas phase reactions are the most popular for the production of petrochemicals and large volume intermediates.

The reaction rate equation is seldom known even for the most experienced reactions. Kinetic equations reported in the literature are usually valid for a specific catalyst, the proprietary formulation, composition, manufacturing technology and morphology making the difference.

3.1.1.1. Experimental reactors. Kinetic experiments are generally carried out in single pass tubular isothermal reactors even if other types of reactors can be used (Fig. 7).

To keep the interpretation as simple as possible the flow is considered to be perfectly ordered with uniform velocity.

This requires sufficiently high velocity and a ratio of tube to particle diameter of at least ten to avoid too much circuiting along the wall.

Small particle diameter also helps in reducing diffusion effects in the catalyst pellets.

Although computers have enabled to handle non-isothermal situations, isothermal conditions are preferred and these are approximated by heat exchange at the wall and, for highly exothermic reactions, by dilution of the catalyst bed.
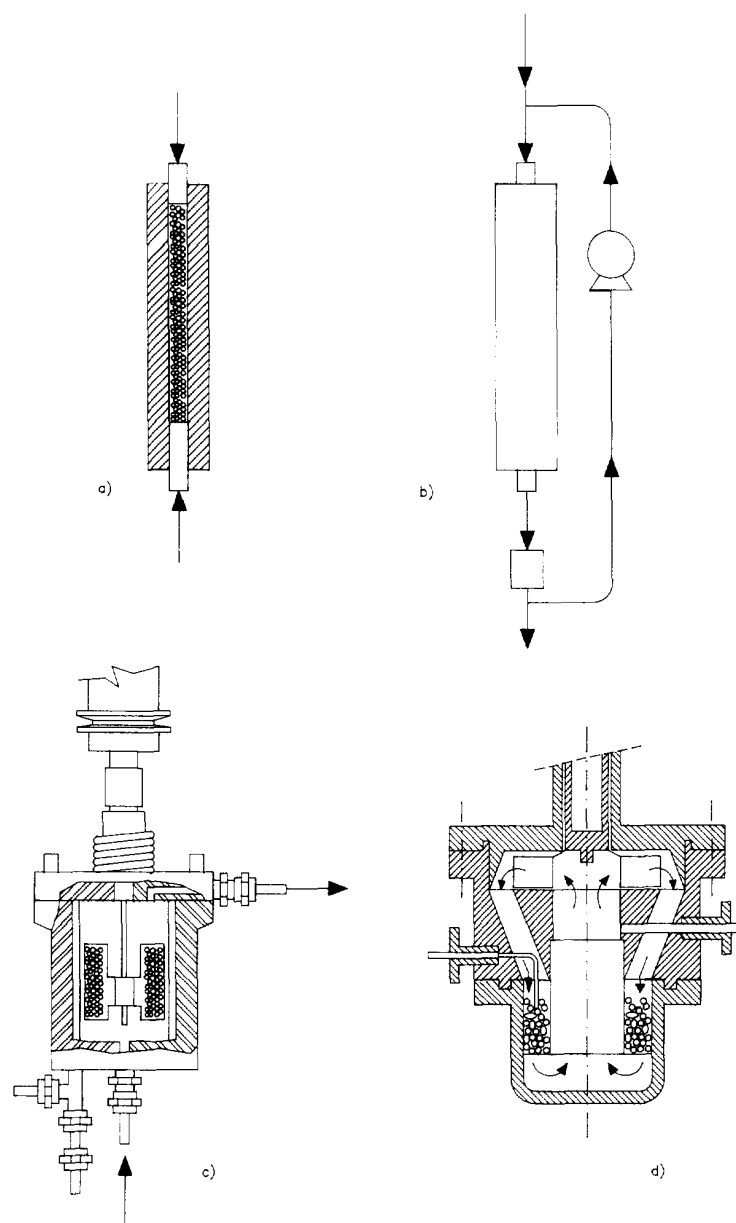
Fig. 7. Various types of experimental reactors. (a) Tubular reactor, (b) tubular reactor with recycle, (c) spinning basket reactor and (d) reactor with internal recycle.

3.1.1.2. Analysis of experiments. If the reactor is designed and operated in an integral and isothermal way, that is with relatively high conversions, the balance equations are very simple:

$$\frac{dX_j}{d\tau} = \mathcal{R}(X,T,P) \tag{3.1}$$

A series of experiments have been carried out in order to cover the experimental space of industrial
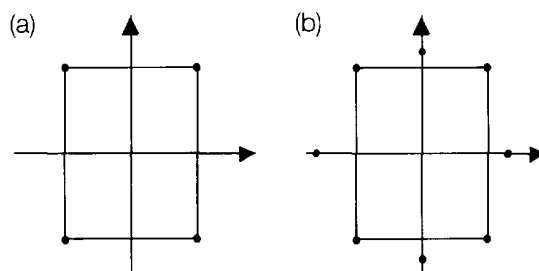
Fig. 8. (a) Factorial design two variables. (b) Centralised composite design (two variables).

interest as far as independent variables, inlet concentrations X_i, temperature T, pressure P and dependent variables, outlet concentrations X_u, are concerned.

Experiments could be planned following patterns such as factorial, fractional factorial or centralized composite designs and could also be arranged sequentially [6,20] (Fig. 8).

The reaction rate $\mathscr{R}$ can be of the Hougen–Watson type and can be derived by the Langmuir–Hinshelwood approach or can be built by automatic selection procedures based on the best fitting of data [11].

For example for the simple reaction

A + B = C + D
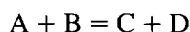
a typical expression is a fractional form of the type

$$\mathscr{R} = \frac{ke^{-E/RT}\left(p_A p_B - \dfrac{p_\epsilon p_D}{K_e}\right)}{1 + K_1 e^{-E_1/RT}p_A + \ldots\ldots\ldots}$$ (3.2)

The numerical integration of Eq. [3.1] and the fitting of computed responses X to experimental values X_e by non-linear least squares (OPTREG), easily determines kinetic parameters K and E [10,14].

3.1.1.3. Modeling the industrial reactor. The availability of a kinetic model is the starting point for scaling up from laboratory to industrial reactors. The way to the industrial one may be however very long.

Several points have to be taken into account:

• first of all the selection of the technology: multitubular, adiabatic multilayer, moving or fluidized bed;

• if inter and intra particle diffusion phenomena are relevant, they should be included in the calculation;

• the flow pattern in the porous bed should be carefully investigated;

• catalyst aging and system stability are to be examined in view of the operation of the plant.

All this problems are treated in the literature and well known in engineering practice. However the method offered in scientific papers is often too cumbersome to be of use in practice and rules derived from experience are often too rough for our scope.

We will leave some of these problems to the examples and focus here the attention on the important phenomenon of diffusion and effectiveness factor in catalyst pellets to demonstrate the level of complexity needed for practical purposes.
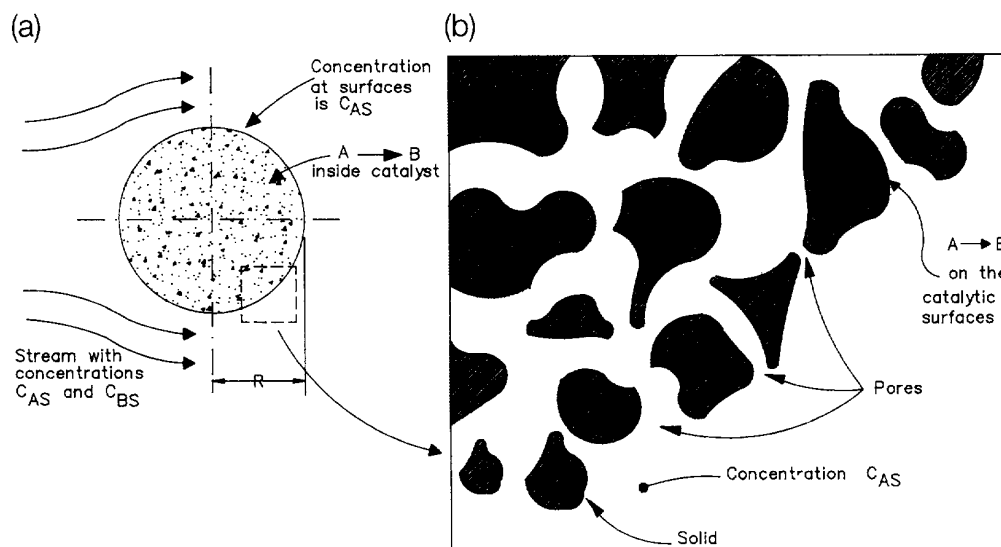
Fig. 9. Spherical catalyst particle, which is porous. Pores in the catalyst in which diffusion

3.1.1.4. Diffusion in a porous catalyst. When reaction occurs on the pore walls of a catalyst pellet diffusion and reaction are linked together. Comprehensive discussions are available in Satterfield [44] and Aris [1].

Aris also shows for first order reactions the influence of particle shape and Dente [19,18,42] proposed and accomplished new shapes in order to improve the efficiency of some reactions.

Froment and Bishoff [27] show how simple particle geometry can be unified with the concept of asymptotic coincidence (Fig. 9).

The assumptions we propose [24] for the computation of grain efficiency are the following:

• grains are spherical with uniform diameter;
• grains are isothermal;
• the diffusion is a multicomponent one.

The mass balance into the grain is:

$$\frac{1}{r^2} \frac{d(r^2 N_i)}{dr} = \nu_i \mathscr{R} \tag{3.3}$$

where $\mathscr{R}$ is the reaction rate and N_i the molar flux

$$N_i = -C_{tot} D_{i,eff} \frac{dx_i}{dr} \tag{3.4}$$

$$D_{i,eff} = \frac{\vartheta}{\tau} D_{i,m} \tag{3.5}$$

where x_i is the molar fraction and C_{tot} the total concentration.

The effective diffusivity $D_{i,eff}$ is related to molecular diffusivity $D_{i,m}$ through the void fraction θ and pore tortuosity τ.

The computation of the molecular diffusivity can be obtained with the aid of Stefan–Maxwell equation [5] together with stoichiometry.

$$D_{i,m} = \frac{\nu_i}{\sum_{j=1}^{n} \frac{(\nu_i x_j - \nu_j x_i)}{D_{ij}}}$$

(3.6)

The linear diffusion coefficients can be computed with the Fuller et al. [28] equations

$$D_{ij} = D_{ij}^* \left(\frac{T}{T_0}\right)^{1.75} \frac{1}{P}$$

(3.7)

The balance equation can be transformed in:

$$C_{tot} D_{i,eff} \frac{1}{r^2} \frac{d}{dr}\left(r^2 \frac{dx_i}{dr}\right) = \mathscr{R}$$

(3.8)

No analytical solution is available being the reaction rate expression non linear. Eq. [3.8] is a second order differential equation with boundary conditions and could in principle be numerically integrated during the numerical integration, step by step, of the material balance Eq. [3.5] for the reactor.

This requires a relative long computing time and sometimes implies numerical problems for convergence.

We suggest [4] from a practical point of view the analogy with a first order reaction that has analytical solution through the definition of a Thiele modulus and the calculation of an efficiency factor to correct kinetics.

For an equilibrium reaction rate of the type [3.2] we define the Thiele criterion as:

$$\Phi = \frac{D_p}{2} \sqrt{\frac{\mathscr{R}}{C_{tot}(x_{i,eq} - x_{i,s})D_{i,eff}}}$$

(3.9)

and a non-dimensional variable

$$\gamma = \frac{x_{i,eq} - x_i}{x_{i,eq} - x_{i,s}}$$

(3.10)

Eq. (3.8) can be written in non-dimensional form

$$\frac{1}{\xi^2} \frac{d}{d\xi}\left(\xi^2 \frac{d\gamma}{d\xi}\right) = \Phi^2 \Psi(\gamma)$$

$$\xi = 1 \rightarrow \gamma = 1$$

$$\xi = 0 \rightarrow \frac{d\gamma}{d\xi} = 0$$

(3.11)

and the efficiency can be computed as:
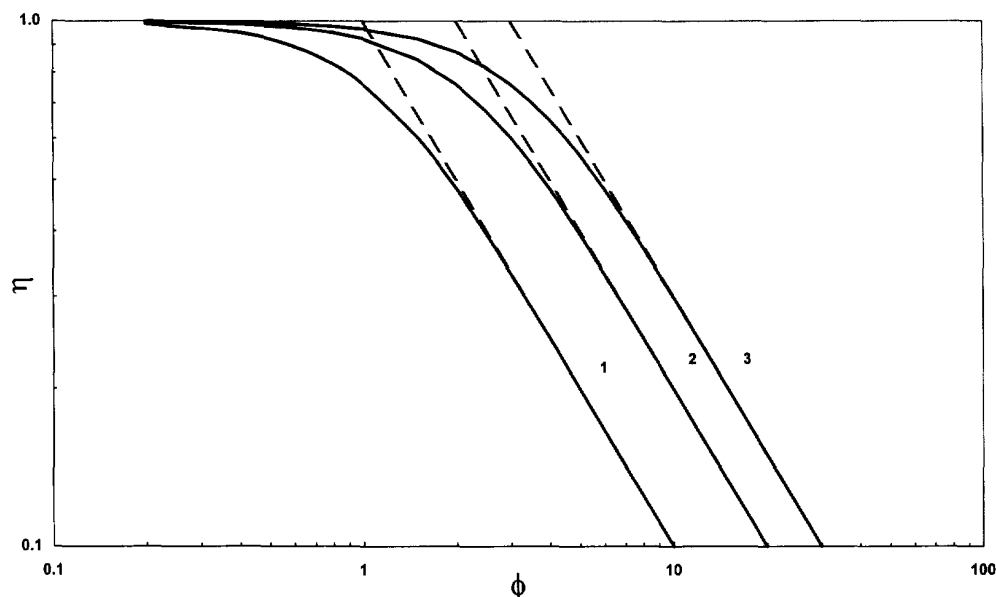
$$\eta = 3\int_0^1 \xi^2 \Psi(\gamma) d\xi$$

(3.12)

Fig. 10. Effectiveness factors for (1) slab, (2) cylinder and (3) sphere (from Aris [1]).

For a first order reaction efficiency can be computed analytically:

$$\eta = \frac{3}{\Phi^2}(\Phi'\text{Coth}\Phi' - 1)$$

(3.13)

The same expression may be used defining a modified Thiele criterion

$$\Phi' = \frac{\Phi}{C^1} = \frac{\Phi}{\sqrt{2}\sqrt{\int_0^1 \Psi(\gamma)\mathrm{d}\gamma}}$$

(3.14)

With a procedure similar to the one used for different pellets geometry (see Fig. 10) and thanks to the modified Thiele criterion, the two asymptotes for $\varnothing \to 0$ and $\varnothing \to \infty$ are exactly computed. In intermediate values error is normally less than 10%.

This is sufficiently acceptable in practical engineering calculations where errors caused by other factors as gas mixture and particle properties are normally larger.

With this example we hope to have shown how there must always be a compromise between calculation, rigorous but still affected by errors and a practical engineering approach in the modeling of reactors.

3.2. Dehydrogenation of ethyl benzene to styrene (An example of scale up from laboratory to industrial reactors)

It may happen that a company is operating industrial plants, built with the support of a licenser of technology, and decides to build larger plants using in-house and consultants skills and experience.

In the case of the styrene synthesis the objectives of the development activity were:
- the obtainment of kinetic equations for different commercial catalysts with the aim of selecting the best one to design the commercial unit;

- evaluating scale up factors and the aging of the catalyst through extensive pilot plant campaigns.
- building a complete mathematical model to compare calculations with existing industrial plant data and use the model to design new reactors.

3.2.1. The synthesis of styrene

The catalytic dehydrogenation of ethylbenzene to styrene is an equilibrium endothermic reaction carried out in gas phase at high temperature (550–600°C). The reaction mean is diluted by important quantities of steam (90–95%) with the scope of shifting thermodynamic equilibrium, reducing the partial pressure of reactants, thus hindering cracking and side reactions, regenerating the catalyst and supplying the heat necessary to the reaction.
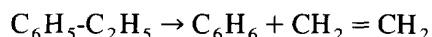
The industrial catalysts are mixtures of iron oxides, chrome, potassium and calcium (SHELL, CCI, GIRDLER).
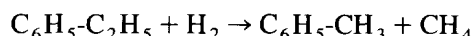
The main and side reactions are the following:

Catalytic dehydrogenation to styrene

$$C_6H_5\text{-}C_2H_5 \rightarrow C_6H_5\text{-}CH = CH_2 + H_2$$
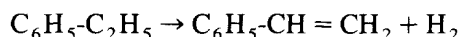
Homogeneous and catalytic dealkylation to benzene

$$C_6H_5\text{-}C_2H_5 \rightarrow C_6H_6 + CH_2 = CH_2$$

Catalytic hydrodealkylation to toluene

$$C_6H_5\text{-}C_2H_5 + H_2 \rightarrow C_6H_5\text{-}CH_3 + CH_4$$

The aging of the catalyst, due to poisoning, loss of active components, coking, breaking, is opposed by an increase in temperature which favors side reactions and accelerates aging.

Experiments and analysis have been organized as reported in Fig. 11.

3.2.2. Micro kinetics

The main effort was first dedicated to the identification of the kinetic equation of styrene formation. A series of preliminary 32 experimental runs, obtained on an isothermal tubular reactor filled with small particles of catalyst (0.6 < d < 1.0 mm) have been used for the scope.

Side reactions have been neglected in this phase of the analysis and the reactor has been assumed to behave ideally.
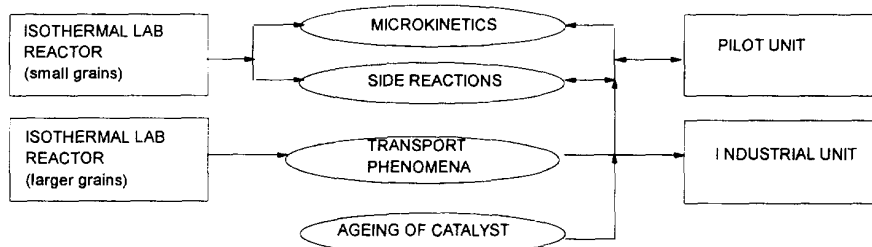

Fig. 11. Synthesis of styrene — organization of experiments and analysis.

Among the several expressions investigated, the following one better fitted experimental data:

$$\mathscr{R}_{STY} = \frac{k_1 e^{-E_1/RT}\left(p_{EB} - \dfrac{p_{STY} p_{H_2}}{K_e}\right)}{1 + k_2 e^{-E_2/RT} p_{EB} + k_3 e^{-E_3/RT} p_{STY}}$$

$$K_e = \exp\left(\frac{-15350}{T} + 16.2\right) \tag{3.15}$$

The reactor has been computed by the balance equation:

$$\frac{dy}{d\tau} = \mathscr{R}_{STY} \tag{3.16}$$

and parameters were found by the minimization of the sum of squares

$$F(K,E) = \sum_{j=1}^{N_s} \left(y_{j,exp} - y_{j,calc}\right)^2 \tag{3.17}$$

The optimization was realized using the OPTREG [7,20] non-linear regression analysis computer program and followed by a statistical analysis of results.

The analysis shows:

• the parameters correlation matrix;
• the variance analysis which gives the error variance computed with the model to be compared to experimental variance from repeated experiments, the determination index that gives the risk to discard the proposed model, the F ratio between the square mean due to regression and the square mean due to error calculated with the model and parameters confidence limits;
• experimental and computed responses and mean and percent errors.

We do not want here to go deeper inside the algorithms used for fitting experimental data and the use of statistics to validate a kinetic model and refer to books [23] and papers [28,9] for more details on this topic.

The importance of efficient regression algorithms and of a sound statistical analysis is never to be forgotten because it gives the necessary confidence in scaling up.

The examined case evidenced correlation between parameters that could be reduced and it suggested, with a procedure similar to that reported in [20], a series of new experiments for a better determination of the parameters.

In order to improve the microkinetics the model has been used to:

• build the kinetic models for secondary homogeneous and heterogeneous reactions;
• validate the assumption of plug flow and absence of important diffusive phenomena.

This was obtained by mathematical analysis followed by additional experiments with diluted catalyst and without catalyst.

The experimental runs at high conversion, necessary to cover the experimental domain and requested by statistical analysis, being impracticable on the laboratory equipment, were simulated by feeding styrene into the reactor.

The scale up from small grains to industrial size catalyst pellets was obtained trough isothermal experiment and the application of the effectiveness model previously shown.

Table 1 shows a comparison of two computed profiles with small particles ($d_p = 0.08$ cm) and large ones ($d_p = 0.7$ cm). One can see that for Thiele modulus equal 0.4 the effectiveness factor (ETA) is nearly 1, while for values of Thiele from 4.2 to 3.3 it varies from 0.5 to 0.6 that is a

Table 1

Computed profiles of Thiele modulus and of effectiveness factor for particle diameter (d_p) 0.08 cm and 0.7 cm.

$\tau = 0.79 \ d_p = 0.08$ cm N. PAS	Thiele	ETA	REFF
1	0.441	0.987	0.013269
2	0.410	0.988	0.011566
3	0.393	0.989	0.010454
4	0.381	0.990	0.009599
5	0.373	0.990	0.008897
6	0.367	0.991	0.008299
7	0.362	0.991	0.007775
8	0.358	0.991	0.007308
9	0.354	0.991	0.006887
10	0.351	0.991	0.006503
$\tau = 0.79 \ d_p = 0.7$ cm N. PAS	THIELE	ETA	REFF
1	4.240	0.540	0.007790
2	3.960	0.566	0.007336
3	3.800	0.582	0.006967
4	3.680	0.594	0.006646
5	3.590	0.603	0.006359
6	3.520	0.610	0.006096
7	3.470	0.616	0.005854
8	3.420	0.621	0.005629
9	3.380	0.626	0.005418
10	3.350	0.630	0.005219

reduction in the reaction rate (REFF) of 40–50%.

Heat exchange and diffusion between the bulk of fluid and the particles surface have also been evaluated and computed but their importance was minimal compared with intraparticle effects.

3.2.3. Pilot scale experiments

The pilot plant used for experiments was a two catalyst layers adiabatic 1 in. I.D. reactor with steam injection between layers as in the industrial case. The reactor has been filled with industrial size catalyst pellets between alumina layers, equipped with thermocouples and sampling devices along the bed and controlled for adiabatic conditions with heat barriers and heating devices to reduce both the exchange coefficient and delta T.

The operation was a continuous one and control, data logging and sampling was realized by a process computer.

The model of the reactor combines three mass balance differential equations and one enthalpy balance.

$$\frac{d\, y_{STY}}{d\tau} = \eta \mathscr{R}_{STY}$$

$$\frac{d\, y_{BEN}}{d\tau} = \mathscr{R}_{BEN_{cat}} + \mathscr{R}_{BEN_{homo}} \frac{\varepsilon}{\rho L}$$

$$\frac{d\, y_{TOL}}{d\tau} = \mathscr{R}_{TOL_{cat}}$$

$$\frac{d(\Sigma y_i H_i)}{d\tau} = 0 \tag{3.18}$$

**EthylBenzene
Conversion**
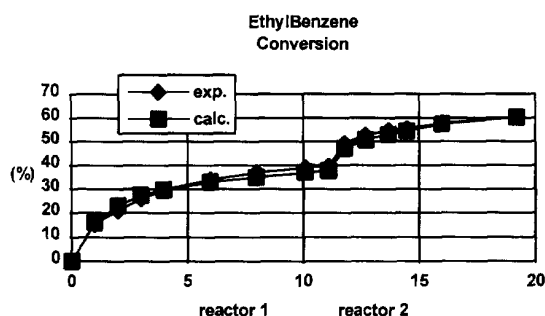
Fig. 12. Ethylbenzene conversion — comparison between computed and measured results.
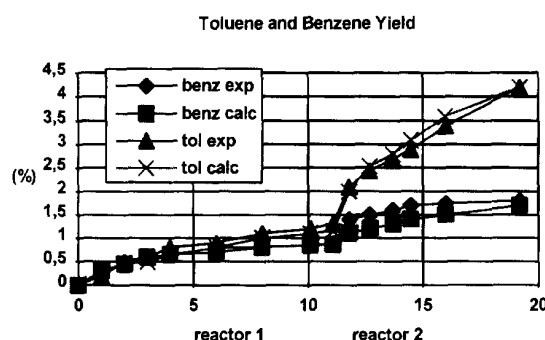
Toluene and Benzene Yield

Fig. 13. Toluene and benzene yield — comparison between computed and measured results.

where y is the molar ratio referred to ethylbenzene feed.

Fig. 12, Fig. 13 and Fig. 14 show a comparison between computed and measured results for a typical sampling in the first 200–400 h of catalyst life (fresh catalyst).

Catalyst aging was investigated over a period of 5000 h that is less than half the catalyst life (13000 h).

The proposed model included the definition of an aging factor F_v as a function of temperature, concentration and their history.

$$F_v = 1 - \int_0^t \exp\left[A + \frac{B}{\mathscr{R}}\left(\frac{1}{T(t)} - \frac{1}{\overline{T}}\right)\right] p_{\mathrm{EB}}(t)\,\mathrm{d}t \qquad (3.19)$$

This factor corrects the catalytic reaction rates and aging parameters are fitted to experimental data.
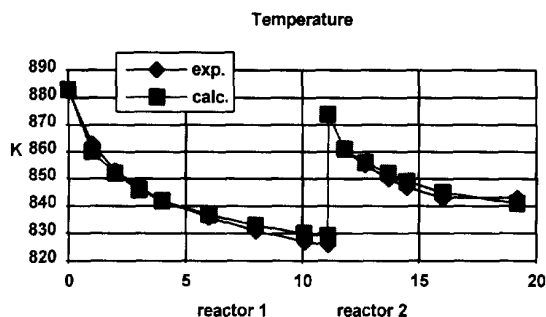
Temperature

Fig. 14. Temperature-comparison between computed and measured results.

The fitting is very good but it is our opinion that such a complex phenomenon should be treated with some caution and the model developed should be continuously revised during the operation of the industrial plant.

The aging phenomenon and model are, in fact, strongly related to the history of industrial plant operation and can be used only if a monitoring of the plant, abnormal conditions included, is available.

3.2.4. Industrial reactor

The application of the model to industrial data had to face a series of problems:

- the availability of complete industrial records was poor and only two campaigns were practically available
- the first data were available in a period between 8500 and 9600 hours of operation and no information had been recorded before and after this period except for an emergency change of 40% of catalyst on the second bed at 7500 h;
- the set of data has been recorded from the start up but operation was stopped at 3500 h for problems on the second reactor.

The fitting of these data with the model, aging factor included, was made possible by the introduction of additional assumptions.

It was however clear to everybody that something was wrong on the second reactor and needed further investigation.

In particular a selection of the initial data of the second campaign revealed some surprising discrepancies between experimental and computed conversions.

The calculation of styrene production was almost exact on the first reactor and in excess of 10–15% on the second one.

Simulated and experimental benzene conversion showed good agreement on both reactors while toluene production, which is mainly catalytic, was computed in excess of 30–40%.

This observations remained qualitatively true for higher time-on-stream experiments.

It is in fact known that catalytic beds having large diameters compared to height may exhibit undesired channeling and flow irregularities if a properly designed distributor is not provided.

A glance to the shape of the two industrial reactors increased this suspect.

In order to take into account these phenomena in the calculations, process engineers use an empirical correction called "catalyst utilization factor" that is a percent of the catalyst really used for the reaction.

To match experimental data on the second reactor an utilization factor 50% was necessary, that is 50% of the catalyst bed was not used in the production process.

The excessively large figure together with the anomalies encountered in the industrial operations forced us to investigate this phenomenon.

The application of the fundamental equations of motion in porous media, that is of continuity equation combined to Darcy law, resulted in the integration of the following differential equations:

$$\nabla(\rho \bar{v}) = 0$$

$$\bar{v} = -\frac{k}{\mu} \nabla P$$

The obtained stream pattern is responsible for flow non uniformity, and the computed dead space was of the same order of magnitude necessary to justify the loss of conversion.

A basis was then available to design new reactors for higher yields and good operation.

3.3. The ammonia synthesis reactor (An existing plant with the need of optimization of operation)

The history of ammonia synthesis dates back to the very beginning of chemical engineering when Haber in Germany and Fauser in Italy made the first experiments to demonstrate the possibility to use atmospheric nitrogen for fertilizers and other applications including dyes and explosives.

The gun barrel where first Fauser performed the reaction departs considerably from the concept of the Fauser–Montecatini multilayer adiabatic reactor with intermediate heat exchange, and from the simpler design of Topsoe having interlayer cold reagent injections.

The idea is very simple and provides a formidable example of scaling up and innovation. The success of the developed reactor technology resulted in applications to other processes. Let us show the basics of this idea with a graphic representation.

The ammonia synthesis reaction is an equilibrium one and the equilibrium line in the conversion–temperature space moves right with increasing pressure.

At a given pressure the operation of the reactor is limited between the activation temperature of the catalyst and the equilibrium line.
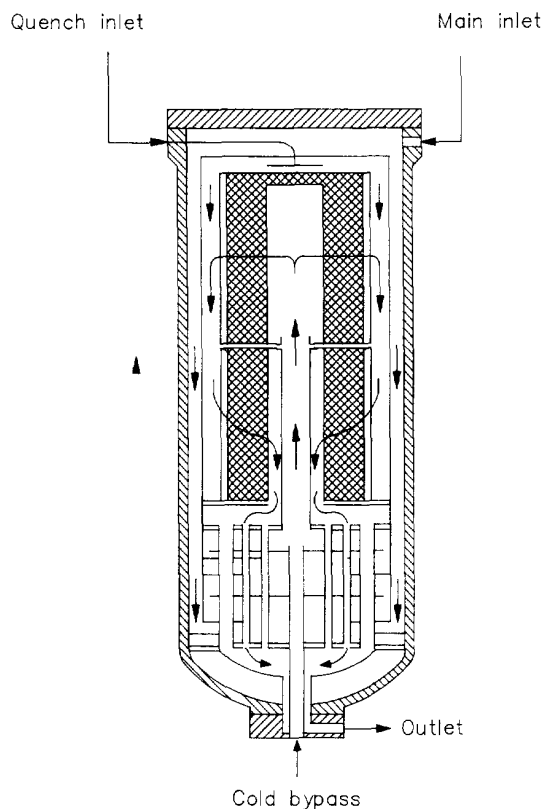

Fig. 15. Modern ammonia synthesis reactors. (a) Radial Haldor Topsoe converter.

Three basic reactor designs can be used for conversions sufficiently high to be industrially practiced:

- very high pressure (1000 bar) adiabatic reactor;
- high pressure (300 bar) isothermal multitubular reactor;
- high pressure (300 bar) staged reactor with intermediate cooling.

The first solution implies high capital and operating costs, the second requires elevated capital costs and the third is the right compromise Fauser found with the limited knowledge of the process available in those days. Topsoe and successively Nielsen refined this concept, simplified the reactor design and improved catalyst performance to come to what is known to be the most popular reactor technology for ammonia synthesis (Fig. 15). The technology is nowadays a very mature one and few things remain on the frontier of innovation:

- new and more active low temperature catalysts
- new materials and reactor concepts.

This breakthrough being far to be achieved, the only possibility is the optimization of today technology design and operation.

A mathematical model approach is presented for the simulation of the industrial unit, stability analysis and optimization.

3.3.1. Mathematical model of the reactor

A lot of work has been done mainly by Nielsen on catalysis and many reaction rate expressions are reported in the literature [41]. As a suitable expression, we have considered the equation of Temkin and Pyzhev [46], in the form proposed by Dyson and Simon [24] and by Buzzi Ferraris and Donati [8,9,11,12].

$$\frac{1}{2}N_2 + \frac{3}{2}H_2 \Leftrightarrow NH_3$$

$$\mathscr{R} = K_0 \exp\left(-\frac{E}{RT}\right)\left\{K_{eq} p_{H_2}\left(\frac{p_{H_2}}{p_{NH_3}}\right)^\beta - \left(\frac{p_{NH_3}}{p_{H_2}}\right)^{(1-\beta)}\right\} \tag{3.20}$$

The values of the kinetic constants and equilibrium expression are those reported in the reference [9].

The computation of grain efficiency was performed with the already presented simplified approach [4].

The examined reactor consists of two adiabatic layers with intermediate supply of cold feed and a heat recuperator as shown in Figs. 16 and 17.

Mass and energy balance were written for the adiabatic layers, the recuperator and cold injection.
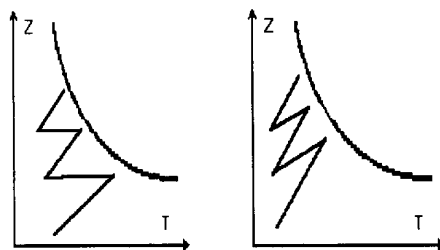

Fig. 16. (left) Conversion vs. temperature; intermediate heat exchangers. (right) Conversion vs. temperature; intermediate cold injections.
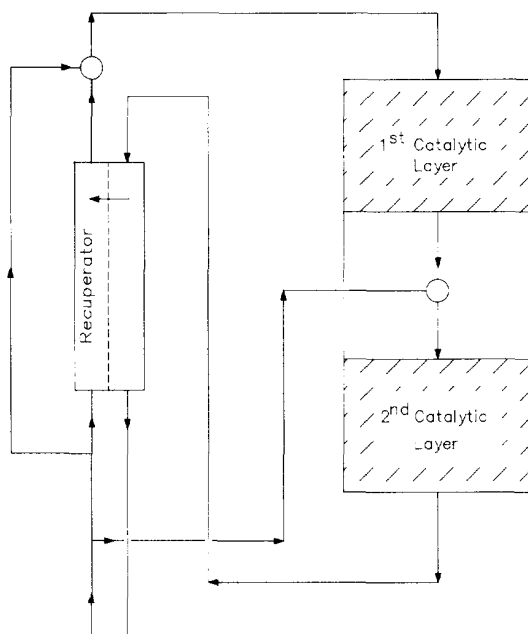
Fig. 17. Scheme of an auto thermal reactor.

The adiabatic layer model was represented by a differential equation for thermal balance and an algebraic equation for mass balance. In case of adiabatic reactors the correlation between temperature and conversion is straightforward.

The differential equation of thermal balance that relates temperature T to the ammonia molar ratio x and to inlet composition x_I

$$W_I \frac{dT}{dV} = \frac{\left(-\Sigma_i \nu_i \tilde{H}_i\right) R_{eff}}{\Sigma_i [X_{iI} + \nu_i (X - X_I)] c_{pi}} \tag{3.21}$$

the algebraic equation for the ammonia molar ratio x

$$X = X_I + \frac{\Sigma_i X_{iI} \left[\tilde{H}_i(T_I, P) - \tilde{H}_i(T, p)\right]}{\Sigma_i \nu_i \tilde{H}_i(T, p)} \tag{3.22}$$

the equations of mass balance that stoichiometrically relate the components of the mixture

$$X_i = X_{iI} + \nu_i(X - X_I) \quad i = 1, \ldots, N$$

We could alternatively write a differential equation for mass and an algebraic equation for enthalpy.

The model of the recuperator is a very simple one. As may be seen in Fig. 17 the warm stream passing through the heat recuperator consists of the whole fluid, whereas the cold stream is only a fraction of it. In fact a part $(\lambda - W_0)$ is directly sent to the second layer and another fraction λ_1 $(1 - \lambda)W_0$ bypasses the heat recuperator providing a mean to control the first layer inlet temperature.

The model is constituted by the following equation:

$$W_0 \Sigma_i x_{i0} \tilde{H}_i(T_0,P) = W_{au} \Sigma_i x_{1,u} \tilde{H}_i(T_3,P) \tag{3.23}$$

$$(1 - \lambda_i)(1 - \lambda)W_0 \Sigma_i x_{i0} \left[\tilde{H}_i(T_1',P) - \tilde{H}_i(T_0,P) \right] = US\Delta T_m \tag{3.24}$$

The intermediate cold injection model was also written in terms of mass and enthalpy balances:

$$W_{i,2I} = \lambda W_0 x_{i0} + (1 - \lambda)W_0 \left[1 + (x_u - x_0)\Sigma_i \nu_j \right] x_{1,1u} \tag{3.25}$$

$$\left[1 + (x_u - x_0)\Sigma_i \nu_j \right](1 - \lambda)W_0 \Sigma_i x_{i,1u} \tilde{H}(T_{1u},P) + \lambda W_0 \Sigma_i x_{i0} H_i(T_0,P)$$

$$= W_0 \left[1 + (x_u - x_0)(1 - \lambda)\Sigma_i \nu_j \right] \Sigma_i x_{i,2I} \tilde{H}_i(T_{2I},P) \tag{3.26}$$

Thermodynamic functions were derived from Hougen, Watson and Ragats [31] with non ideality corrections provided by Maron and Turnbull [37,38].

3.3.2. Stability analysis of the auto thermal system

If we consider the reactor (Fig. 17) alone and look at it as a system that we have to control and to optimize, the variables identifying the feed (flow rate, composition, temperature and pressure) are independent and non controlling. In fact the only free variables (Fig. 18) are the heat recuperator bypass fraction λ_1, and the fraction λ to the second catalytic layer. These two variables are at the operator's disposal both for reactor optimization, and for the stationary state control. The mathematical model of the different sub-systems of the reactor must be able to compute every internal and output conditions for each determination of the input variables and bypass fractions λ_1 and λ. As is well known after Van Heerden [48], this result cannot be reached in one step, because the thermal feedback due to feed preheating by the effluent gas, gives rise to an intrinsically boundary value problem.

The non linearity of the model makes it impossible to solve the problem by a "marching" method and the use of an iterative method is required. We have thought that it was better to change, from both
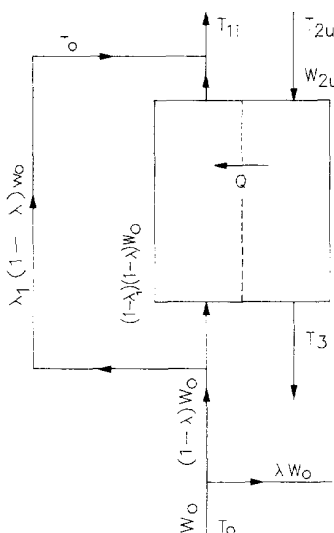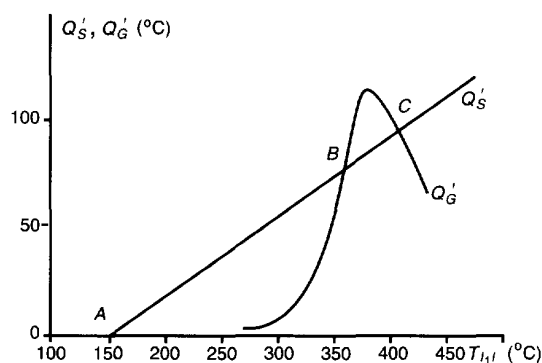

Fig. 18. Scheme of recuperator flows.

Fig. 19. Diagram of heat produced and exchanged vs. inlet temperature in the first bed (values of l and l_t being fixed). Points A and C are stable, point B unstable according to the static criterion.

logical and operational point of view, the variable heat recuperator bypass fraction λ_1, with the variable feed temperature to the first layer T_{i1}. In this way it is possible to open the internal reactor loop and to compute the layers, the injection and finally the amount of heat generated and exchanged; these two last terms appear in Eq. [3.24] of thermal balance on the recuperator. For a given value λ, the study of the intersections of the two quantities mentioned before as a function of temperature T_{i1} constitutes the basis for the system stability analysis according to the Van Heerden stationary criterion (see Fig. 19 in which both generated and exchanged heats are plotted in terms of temperature differences against temperature T_{i1}).

By this change in the operational variables, it is possible to find a stationary state point, if it exists, without iterating the computation of the adiabatic layers. This iteration in fact would require a certain amount of computing time. On the other hand it is enough to iterate the recuperator equation that requires shorter computing time. In our opinion this is important; actually, if we look for the optimal operating conditions, the model must be computed several times in order to reach the optimum by a direct method. In this case, the developed computing procedure, using as optimization variables λ and T_{i1} instead of λ_1 and λ, avoids a double iteration cycle.

In this way, we have tackled both the reactor partial optimization problem (with the use of the two decision system variables) and the analysis of stability at the operating point found.

Before examining the optimization algorithm, let us make some observations on the stability analysis. The need of controlling and of optimizing the reactor during its operations arises from the existence of disturbances on the independent input system variables (feed). The consequence of these disturbances is that the reactor leaves the optimal conditions previously attained and it is necessary to adjust it to a new optimal point. During optimization, we must control the danger to reach blow-out points. The optimal operation point and the extinction (unstable) point, as other AA. already remarked [48,45], are fairly close one to the other.

We have adopted two rules that, during optimization, can be used, either separately or together. The first consists in the comparison between the derivative of the generated and exchanged heat functions to temperature T_{i1} computed at the operating point (see Fig. 19). It can be numerically done with only an additional reactor computation.

The second rule consists in the approximate evaluation of the extinction point and the computation of its distance (in terms of temperature T_{i1} and bypass fraction λ_1) from the operating point found by

us. These two differences ΔT and $\Delta\lambda$ must be systematically compared with the values that simulation and sensitivity off-line studies, information on the instrumentation degree of confidence and overall control experience, have proved to be reasonable. It may be convenient to make further observations about the strategy used, which was experimented only for simulated cases. Under normal operating conditions, the optimization program looks for the optimal point without taking into account the reactor stability. For this research a certain number of iterations are used (objective function evaluations). Afterwards the main program computes the distance between the actual point and the blow-out point (second rule). This requires three or four reactor mathematical model computations. If the comparison with the reference values is positive we accept the point; in the opposite case the optimization program starts a new calculation cycle using an objective function that is penalized by the degree of proximity at the unstable point measured by the first rule. Other options are at the operator's disposal if he wants to intervene directly.

3.3.3. Optimization program used

The program of process optimization exhibits some peculiarities that require the study of a special optimization algorithm. The reasons conditioning the optimized structure are, for a large number of on-line optimization problems, essentially the following: (1) process computers have small dimensions and (2) a large number of computations cannot be devoted to the search of optimal conditions.

Small computers are generally used in an industrial unit and they accomplish several services, such as the solution of mass balance equations, the regulator control etc.: these tasks cover a great part of the available computing time. The introduction of on-line optimizers is reasonable, if by taking into account the aforementioned functions, there is enough time and memory space, and the intervention time is consistent with the frequency of the disturbances. No matter how synthetic and ingenious the mathematical model is, a considerable amount of computer time and memory is employed during optimization.

We understand the necessity to have a particularly compact optimization program. Due to the above reasons and in order to obtain the most convenient on-line optimize intervention, it is not possible to devote a great number of computations to the objective function. Then a very complex program is not required (as it may be a general optimization program), but it is necessary to improve the objective function as fast as possible for the given number of function evaluations. If, on the other hand, we consider the fact that the program works again and again on the process and that the optimal conditions change during optimization, we can reasonably say that the attainment of the mathematical optimum may have only a relative interest. These observations led us to the building of a program for on-line optimization of industrial units.

Among the various efficient criteria reported in literature [7,3], which do not require a great memory occupation, we have chosen those proposed by Hooke and Jeeves [30] and by Spandley (Simplex) in the version modified by Nelder and Mead [40]. The proposed algorithm results by the proper union of the two criteria with the purpose to profit by the advantages of both. In particular, in the first phase of the search, we use the Hooke and Jeeves method since it is possible to know reasonable values for the independent variables modifications. The first guess values for the search steps can be in fact estimated on the basis of the experience acquired during the previous optimization cycles. The Simplex method, on the other hand, has proved to be useful since it very rapidly modifies the search pattern when the initial step guess values were not proper.

The constraints of the independent variables were handled by penalizing the objective function with weights depending on the local values of the function and of the constraints.

Table 2

Data concerning the two-bed adiabatic reactor, the recuperator at the normal operating conditions

	1st Bed		2nd Bed
Volume of the bed	$7.7 \ m^3$		$15.4 \ m^3$
Diameter of the grains	5 mm		3 mm
Porosity of the bed	0.46		0.46
Surface of the recupertor	850		m^2
Total Feed (G)	$2.75 < ts > 10^5$		kg/h
Feed composition (molar fractions)	x_{H2}		$= 0.21$
	x_{N2}		$= 0.63$
	x_{CH4}		$= 0.09$
	x_{NH3}		$= 0.04$
	x_A		$= 0.03$
Inlet temperature of the recuperator (T)	150	°C	
Pressure (P)	250	atm	
Level of the perturbed variables	0	+	
$G \ (10^{-5} \ kg/h)$	2.2	2.75	3.3
T (°C)	140	150	170
P (atm)	230	250	270
Production under nominal conditions (NH_3 t/day)			1.100

3.3.4. Simulation experience

With the aid of the mathematical model and of the optimization algorithm, a certain number of simulation trials have been performed. These experiments are similar to those that should be done by the process optimizer during the operation of the industrial unit to make it work under optimal and stable conditions.

The results reported concern the reactor alone (its characteristics are represented in Table 2). Table 3 shows the results obtained for the simulations of the disturbances on the unit input variables:

- the levels of the input variables, the initial and final value (after 50 optimization program iterations) of the objective function F (tons of NH_3, per day);
- the number of iterations required in order to increase the objective function to 80% and 95%;
- the optimal values of the first layer feed temperature T_{i1} and the values of the bypass fractions λ and λ_1.

Table 3

Results of the calculations

| Run	P	T	G	F initial	F final (50 iterations)	n. iterations 80% F	n. iterations 95% F	T_n (°C) final	λ final	$\lambda 1$ final
1	0	0	0	1089.0	1106.0	9	11	408.7	0.3015	0.2104
2	−	−	−	878.8	882.3	15	19	400.7	0.2968	0.2206
3	−	−	+	969.2	1179.0	16	20	429.4	0.2671	0.0817
4	−	+	−	803.1	878.2	17	35	396.9	0.3151	0.2819
5	−	+	+	934.8	1175.0	17	28	427.0	0.2851	0.1382
6	+	−	−	896.4	990.9	20	31	303.4	0.3451	0.2701
7	+	−	+	1115.0	1342.0	15	19	416.6	0.2056	0.1729
8	+	+	−	905.7	987.8	18	34	386.4	0.3527	0.3380
9	+	+	+	1054.0	1337.0	17	20	414.0	0.3167	0.2221
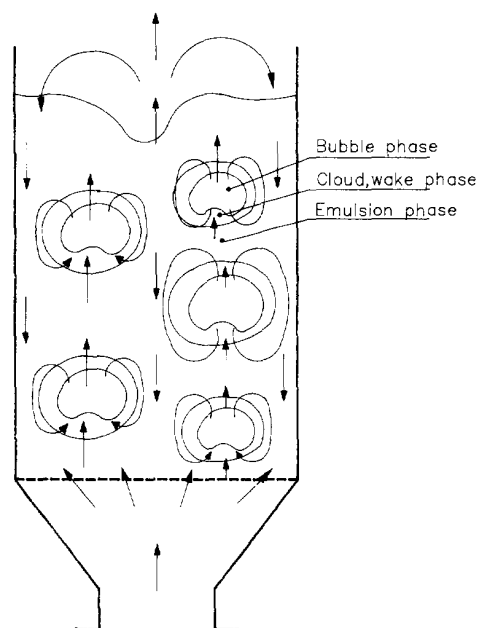
Fig. 20. The fluidized bed according to the three phases model.

All operating points are stable according to the static criterion; nevertheless some of them are very close to the extinction conditions.

For the present case all the adaptive factors that take into account the slow drifts of the unit (aging and poisoning of the catalyst etc.) were fixed at their nominal values.

3.3.5. Fluidized bed reactors (a tentative scale up)

Even though the rational design of fluidized beds is not completely established at the present time, some aspects have been studied extensively and are summarized in the books of Leva [36] Zenz and Othmer [51], Davidson and Harrison and Kunii and Levenspiel [17,35].

One of the major complications in developing a mathematical model of a fluidized bed is that experimental observations seem to indicate that, in a wide range of gas velocities, two distinct regions exists in the bed:

- a dense region with a large fraction of particles;
- a dilute or bubble phase.

With reference to Fig. 20 bubbles are formed at the distributor, move upward and in this motion they lift a certain quantity of solids (cloud and wake) generating a mixing and a powder recirculation in the bed.

Gas permeates the dense phase or emulsion and is transferred from bubbles to cloud and to the emulsion phase.

A simple single-dispersion to represent gas and solid mixing has not been successfully correlated in a general fashion to the extent that adequate predictions can be extracted. It is therefore a risk to use them for scaling up.

A number of models all having dense and bubble phases have been proposed.

The two phase models consider bubbles and emulsion and different combinations of flow patterns, plug, completely mixed.

Even if they do not justify the real motion of solids and the downward motion of gas together with solids at sufficiently high gas superficial velocity, they are simple to compute and closer than dispersion models to reality and can be used to provide an idea of the reactor performance in some situations.

Too many assumptions are however used to define model parameters to be confident in their reliability.

The models used by Davidson et al. and by Kunii–Levenspiel are based on a physical picture closely related to the hydrodynamics of the bubble motion, but nevertheless bubble diameter cannot be accurately predicted.

In addition real fluidized bed have different distributors, may be provided with baffles and internals that break bubbles and modify the flow pattern and usually operate in the fast fluidization regime that is hardly represented by the Davidson picture.

Given these difficulties that can be solved only by experiments on mock-ups and by experienced acceptance of the scale up risk, we will show how easily can be built the most complex three phase model and how can be used for sensitivity analysis.

3.3.6. The three phase model

The three phases model (Fig. 20), as developed by Kunii and Levenspiel [35] and by Freyer and Potter [26], takes into account in a phenomenological way the back mixing of solids and gas in fluidized beds.

The solids lifted by bubbles are in fact released at the top of the bed and fall back in the emulsion phase. If this movement is sufficiently high, for fluidization velocities greater than a critical value $(u > u_{cr})$, the gas changes direction in the emulsion phase and crosses the solids downwards.
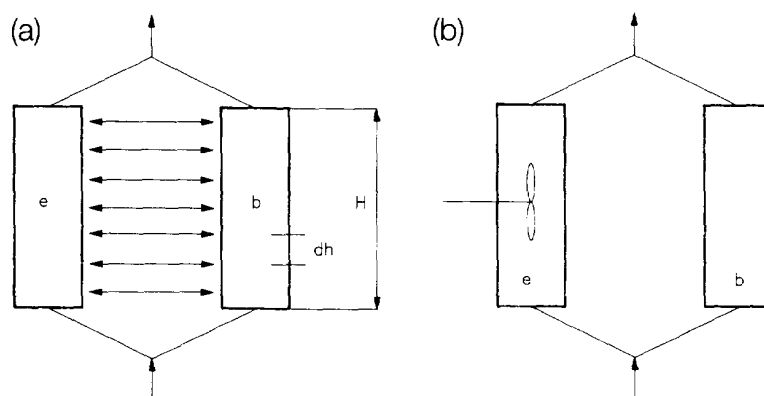

Fig. 21. (a) Two phase model with crossflow between phases, both plug flow. (b) Two phase model with perfectly mixed emulsion phase and plug flow bubble phase.
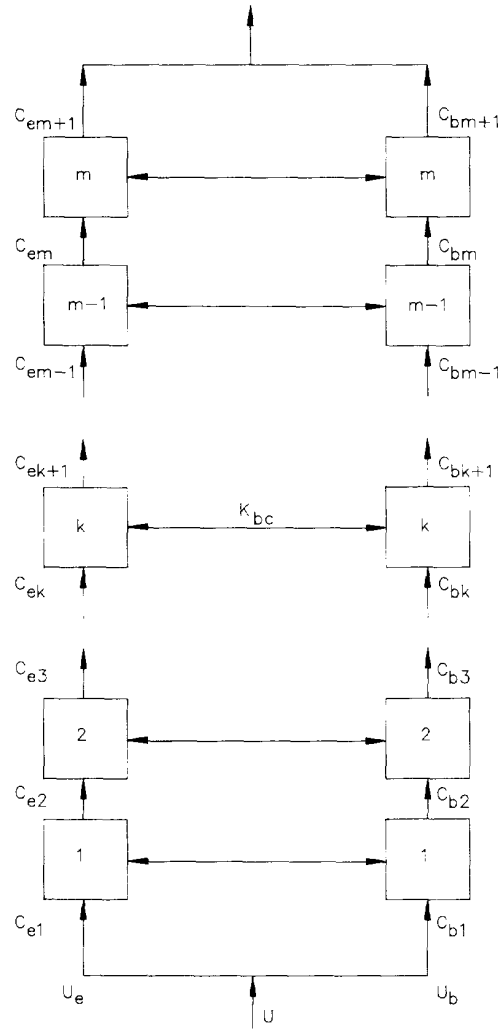
Fig. 22. Two phase model — Unit cell approach.

With reference to cell model in Figs. 21–24 and assuming u constant the mass balance for a cell height dh can be written in terms of concentrations C_i:

$$-\frac{dC_{bi}}{dh} = \left[k_{bci}(C_{bi} - C_{ci})\delta \right]/u_b$$

$$-\frac{dC_{ci}}{dh} = \left[k_{cei}(C_{ci} - C_{ei})\delta - k_{bci}(C_{bi} - C_{ci})\delta + \left(\sum_{j=1}^{N_R} \nu_{ij}\mathscr{R}_{cj} \right) f_w \delta \right]$$

$$-\frac{dC_{ei}}{dh} = \left[-k_{cei}(C_{ci} - C_{ei})\delta - \left(\sum_{j=1}^{N_R} \nu_{ij}\mathscr{R}_{cj} \right)(1 - \delta(1 + f_w)) \right]/u_e$$
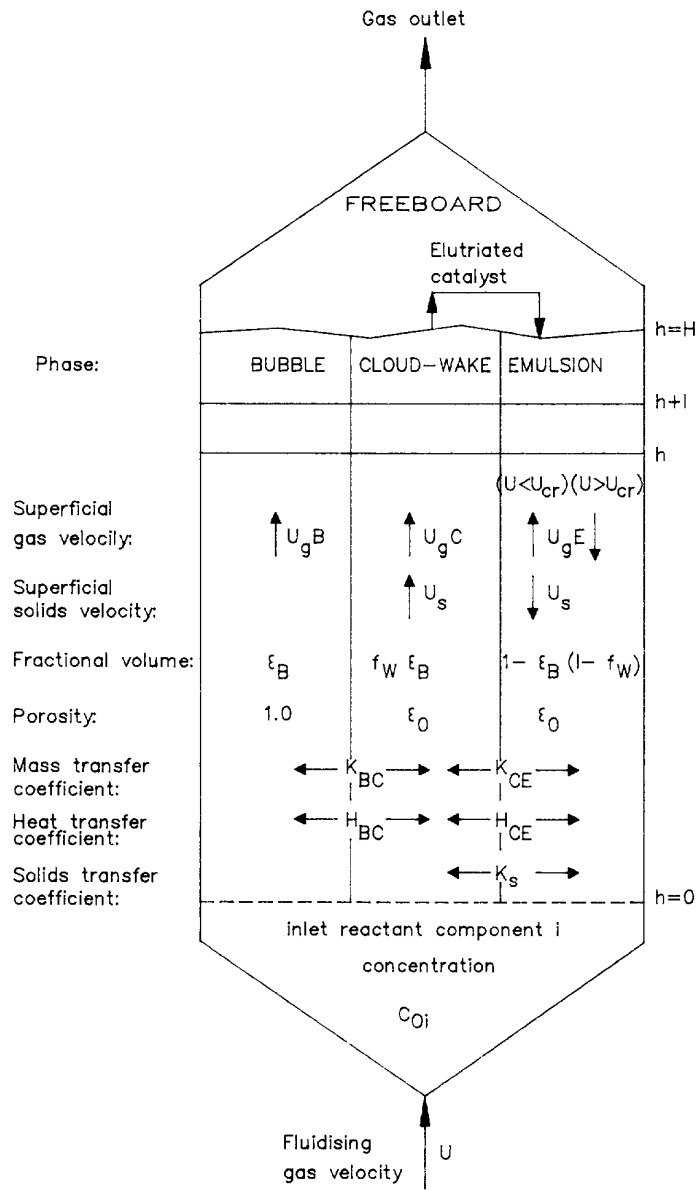
Fig. 23. Three phase model.

with the boundary conditions:

$$\text{backmixing}\begin{cases} h = 0; C_{bi} = C_i^0; -u_e C_{ei} + (u - u_b)C_i^0 = u_c C_{ci} \\ h = H; C_{ei} = C_{ci}; C_i^H u = u_b C_{bi} + (u - u_b)C_i \end{cases}$$

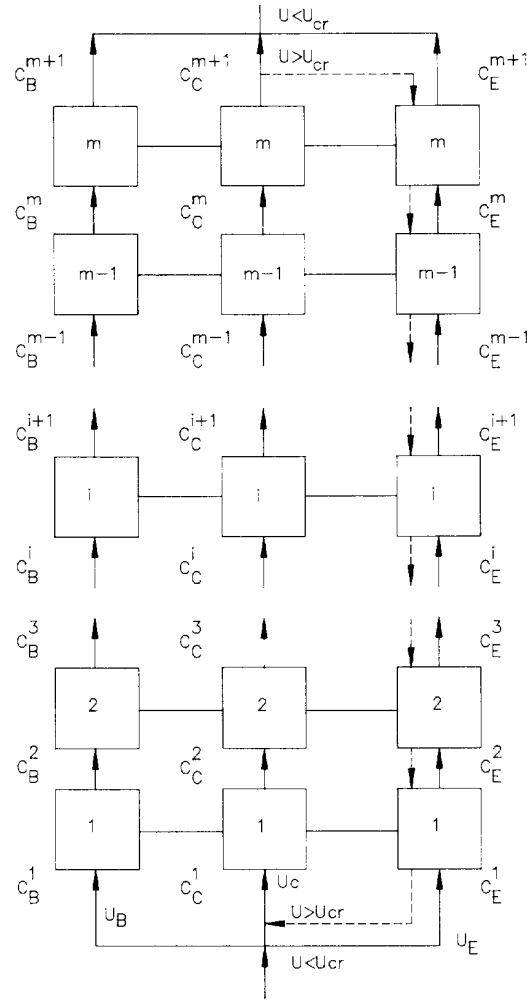$$u < u_{cr}\{h = 0; C_{bi} = C_{ei} = C_{ci} = C_i^0.$$

Fig. 24. Three phase model. Unit cell approach.

The mass transport coefficients are computed using the equations that Davidson and Harrison have derived from Higbie penetration theory:

$$K_{bc} = 4.5\left(\frac{u_{mf}}{d_b}\right) + 5.85\left(\frac{D^{1/2}g^{1/4}}{d_b^{5/4}}\right) \tag{3.27}$$

$$K_{ce} = 6.78\left(\frac{\varepsilon_{mf}D_j u_b}{d_b^3}\right)^{1/2} \tag{3.28}$$

The bubble velocity has been computed by:

$$u_b = u - u_{mf} + 0.711(gd_b)^{1/2} \tag{3.29}$$

The minimum fluidization velocity U_{mf} has been evaluated with the empirical correlation derived from experiments:

$$Re_{mf} = \sqrt{33.7^2 + 0.0408\,N_{GA}} - 33.7 \tag{3.30}$$

$$Re_{mf} = \frac{d_p u_{mf} \rho_g}{\mu}; \quad Re_{mf} \leq 3000 \tag{3.31}$$

Bubble diameter was assigned or evaluated with the expression available for the maximum bubble diameter.

$$D_b = (u_t/0.71)^2 \frac{1}{g} \tag{3.32}$$

Cloud to bubble fraction f_w and bubble fraction δ in the bed were computed as velocity ratios:

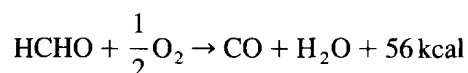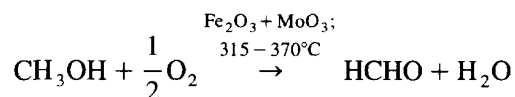$$f_w = \frac{3u_f}{u_b - u_f} \tag{3.33}$$

$$\delta = \frac{u_b'}{u_b} \tag{3.34}$$

where u_b' is the superficial bubble velocity.

The solution of the resulting system of non linear equation was obtained by the SISPAR program mentioned in [21].

3.3.7. A possible application

Let us suppose we wish to evaluate the possibility of application of the fluidized bed technology to a well known reaction as the formaldehyde synthesis where heat effects and mixing could result in some advantage in the reactor operation.

$$CH_3OH + \frac{1}{2}O_2 \xrightarrow[]{\overset{Fe_2O_3 + MoO_3;}{315-370°C}} HCHO + H_2O$$

$$HCHO + \frac{1}{2}O_2 \to CO + H_2O + 56\,kcal$$

$$\mathscr{R}_1 = 3.3 \cdot 10^5 \exp\left(-\frac{8850}{T}\right) \frac{C_{O_2}^{1/2}\,C_{CH_3OH}^{1/2}}{C_{O_2}^{1/2} + 0.5\,C_{CH_3OH}^{1/2}} \left(\frac{T}{700}\right)$$

$$\mathscr{R}_2 = 2.46 \cdot 10^5 \exp\left(-\frac{8025}{T}\right) C_{CH_2O}\left(\frac{T}{700}\right)$$

$d_p = 0.2\,mm$; $\rho_v = 1.0\,g/cm^3$; $\varepsilon_{mf} = 0.6$; $PM = 29.0\,g/mol$

$T = 250°C$; $P = 1.6\,ata$;

$C_{CH_3OH}^0 = 0.21 \cdot 10^{-5}\,mol/cm^3$

$C_{O_2}^0 = 0.656 \cdot 10^{-5}\,mol/cm^3$

$\mu = 0.00028\,poise$; $D_i = 0.17\,cm^2/s$

Table 4
Conversion and selectivity for different fluidized bed models

Model	Methanol Conversion (%)	Conversion to Formaldehyde (%)	Selectivity
Two Phases			
Bubble phase plug-flow emulsion – 1 stage	89.31	85.95	96.20
Bubble phase plug-flow emulsion – 29 stages	90.16	87.08	96.50
Bubble phase and. emulsion – 1 stage	85.94	81.88	96.20
Bubble phase and emulsion – 29 stages	89.64	85.64	95.6
Three phases	78.70	76.00	96.50

The most important results of industrial interest are conversion and selectivity. Table 4 reports a synthesis of the results obtained for the assumed reactor schematization and, as far as selectivity is concerned, gives figures very near to those obtained in the traditional multitubular plug flow reactor.

4. Gas liquid reactors

There are many examples of reactions between gases and liquids in industry. They belong to two categories. The first one groups the gas purification processes like CO_2, H_2S, NO_x removal from process streams. The second category is related to many production processes like carbonylation, carboxylation, oxidation, hydrogenation, chlorination and also polymerization and fermentation. This reaction technology covers a large share of production of fine chemicals and large volume intermediates from antibiotics, to dyes, additives, large volume and well known intermediates such as phenol, caprolactam, adipic acid, terephtalic acid and esters, acetaldehyde, oxoalcohols, hydrogen peroxide etc.

These processes are carried out in a variety of equipment ranging from bubbling absorbers, to packed or plate columns, to stirred autoclaves, to airlift or jet loop reactors.

The importance of technology with respect to reactor performance has been often overlooked and this is in many cases the reason of poor process performances.

It has already been remarked in the introduction that reaction rate is strictly related to the gas liquid interphase area and that, being in most cases the reaction rate very fast compared to liquid phase diffusion, the reactor volume effectively used is limited to a thin layer surrounding bubbles.

This concept has been extensively investigated by Witman [50], Westerterp [34], Bird [5], Danckwerts [16], Astarita [2] and we suggest for a comprehensive approach chapter 6 of the book by Froment and Bischoff [27].

As it will be clear from the examples, the theory is very similar to that developed for gas solid reactions with the exception that diffusivity is much lower and this is the basic reason why a gas liquid reactor needs higher residence times for a given conversion.

The example is taken from industrial experience of debottlenecking a batch emulsion polymerization suffering from a poor technology [52].

It will be clear that the role of kinetics is far less important than that of fluid dynamics and mass transfer. The difficulty of lack of theoretical approaches in predicting gas liquid interphase area, hence in scaling up, is overcome by appropriate experiments.

4.1. Impeller selection ad scale up of an emulsion polymerization

The emulsion polymerization of a gaseous monomer to yield a valuable commercial product is a complex problem from many points of view.

If one wants to go deep into all the involved elementary phenomena, one is faced by a combination of problems in fluid mechanics, turbulent diffusion, chemical kinetics, particle growth, interphase and intraphase heat and mass transfer, and so on.

Extensive experimental and theoretical work is necessary, which often contrasts with pressing production. In this situation the need for an engineering approach is obvious.

In many cases the analysis of the system, made in cooperation with the experts in the field, can lead to the selection of the most important phenomena and finally to a strategy of solution in terms of a few basic ideas, which can be developed by means of relatively low cost experiments.

This work shows how it is possible to characterize an emulsion polymerization reactor completely and to obtain results of industrial relevance through a series of fluid dynamic experiments performed on reactor models at various scales and using both the industrial emulsion and very simple reacting systems.

4.1.1. Statement of the Problem

The emulsion polymerization is carried out in stirred unbaffled reactors.

The industrial facilities include a pilot 50 l autoclave, the aim of which is testing various polymerization recipes, experimenting different process conditions and developing new products. Gaseous monomer is sent into the ceiling of the reactor. The polymer grows under stirring as a particulate dispersion in water originating an emulsion, the concentration of which increases with time.

The polymerization reaction is exothermic and temperature is controlled by cold water in the jacket. Pressure can be varied to control reaction rate.

At the start-up of production a lot of problems became evident regarding monomer purity, catalyst addition policy, the type and quantity of chemicals to be used, temperature and pressure level. Some of these problems were solved by research chemists and plant operators.

The productivity and emulsion concentration achieved in the pilot plant were however not reproduced in the industrial autoclave which exhibited lower performances.

In the industrial reactor, in order to have an acceptable polymerization rate, intense agitation was needed, because an increase in the stirrer speed causes an increase in the overall rate. However intense agitation has a negative effect on the stability of the emulsion.

On the basis of these simple observations the study was focused on the fluid dynamic effects on emulsion stability and reactor productivity.

Namely a stirring device had to be studied having a low shear on the emulsion for stability and suitable to be easily scaled up from the pilot to the industrial autoclave for productivity.

4.1.1.1. Basic concepts. Since a scale-up at constant productivity has to be made, the polymerization overall rate must be examined.

Generally speaking, for a gas–liquid reaction the overall reaction rate (macro kinetics) is due to two combined processes:
- diffusion of the gaseous reactant within the liquid phase (mass transfer):
- reaction in the liquid phase (micro kinetics).

The first step is strongly influenced by fluid dynamics while the micro kinetics depend only on the local state variables.

Following Calderbank [15] three regimes may be considered:

- very slow kinetics where the chemical reaction rate is rate determining;
- fast reaction rate where diffusion controls the overall rate;
- very fast reaction in which material transfer is increased due to the chemical reaction in the diffusion zone.

In the last case if the reaction is of first order and irreversible the overall rate depends on fluid dynamics only through the interphase contact area but is independent of the mass transfer coefficient.

Since the polymerization studied is a very fast reaction, with the assumption of first order with respect to monomer concentration, it may be inferred that the interphase area per unit volume of the reactor must be scaled up if the same productivity has to be obtained.

The total interphase contact area in the unbaffled reactor consists in the surface of the vortex and, if the speed of the stirrer is high enough, in the surface of bubbles generated by the cavitation of the blades.

It is apparent that the interphase area per unit volume is strongly influenced by the reactor scale and by the impeller type and speed.

In order to determine this influence a series of experiments was performed at the laboratory and pilot scale with different types of stirrers and rotational speeds.

The vortex dimension can be measured and computed following Nagata [39], the total interphase area can be determined by the absorption of oxygen in catalyzed sodium sulfite solutions following Westerterp [49].

For the agitation conditions examined, emulsion stability can be evaluated by degradation tests on the industrial product.

4.1.2. Fluid dynamic model

4.1.2.1. Vortex dimension.
In a stirred unbaffled reactor the liquid surface is not plane but it assumes the shape of a cone vortex.

The dimensions of the vortex depend on the geometry of the vessel and agitator and on the speed of the stirrer.

The vortex may be stable (Fig. 25a) or unstable due to the fact that it reaches the top of the autoclave (Fig. 25b) or cavitation of the agitator may be present (Fig. 25c) with a spreading of
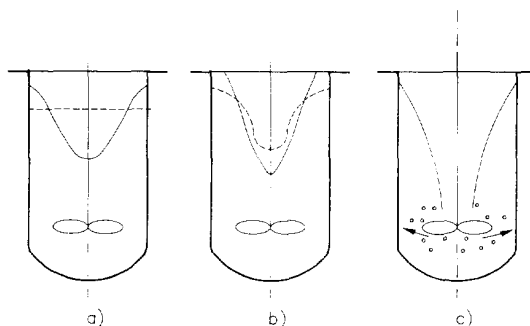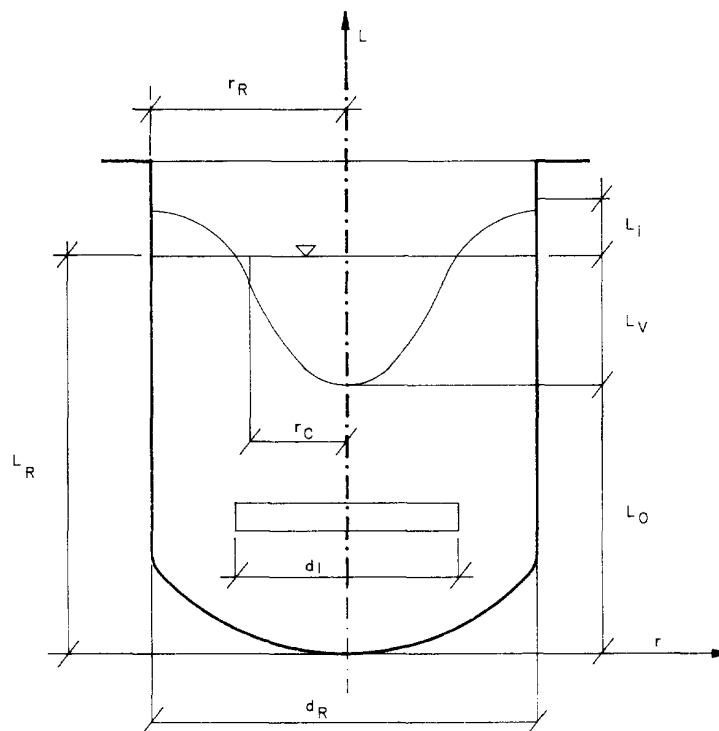

Fig. 25. Unbaffled reactor vortex configurations.

Fig. 26. Reactor scheme and definition of symbols.

bubbles in the liquid. A simple fluid dynamic model that explains vortex formation and the dependence of the shape on the speed of the stirrer, under stable conditions, is given by Nagata [39]. The model assumes for the tangential velocity the following expressions:

$$u_t = \omega r; \quad 0 \leq r \leq r_c \tag{4.1}$$

$$u_t = \frac{\omega r_c^2}{r}; \quad r_c \leq r_R$$

where ω is the angular velocity of the stirrer, r_c is a characteristic radius and r_R is the radius of the vessel.

The shape of the vortex is obtained from [15] applying the condition that the free surface is isobaric.

With the symbols of Fig. 26 the following equations are obtained:

$$L = L_0 + \frac{\omega^2 r^2}{2g}; \quad 0 \leq r < r_c$$

$$L = L_0 + \frac{\omega^2 r_2}{2g}\left[2 - \left(\frac{r_c}{r}\right)^2\right]; \quad r_c \leq r \leq r_R \tag{4.2}$$

The conservation of the liquid volume gives an equation for the vortex depth L_v:

$$L_v = L_R - L_0 = \frac{\omega^2 r^2}{g} \left\{ \left(\frac{r_c}{r_R} \right)^2 - \left(\frac{r_c}{r_R} \right)^4 \left[\ln \left(\frac{r_R}{r_c} \right) + \frac{3}{4} \right] \right\}$$

(4.3)

and for the vortex height:

$$L_l = \frac{\omega^2 r_R^2}{g} \left(\frac{r_c}{r_R} \right)^4 \left[\ln \left(\frac{r_R}{r_c} \right) + \frac{1}{4} \right]$$

(4.4)

From experimental data for L_v (or L_l) it is possible to compute the parameter r_c, which for high Reynolds numbers ($> 40\,000$) is fairly a constant for a given stirrer.

In the case of a stable vortex the interphase area can be easily computed by the following expression:

$$A = 2\pi \left\{ \int_0^{r_c} r \sqrt{\frac{1 + \omega^4 r^2}{g^2}} \, dr + \int_{r_c}^{r_R} r \sqrt{1 + \frac{\omega^4 r_c^8}{g^2 r^6}} \, dr \right\}$$

(4.5)

When cavitation occurs the area of the bubbles generated by agitator is to be added to the area of the vortex given by expression (4.5).

In this case, the global area can be obtained by a series of experiments as the ones described in the following section.

4.1.2.2. Overall interphase contact area.

Given a substance S that diffuses from a phase into a second one, where it is consumed by a first order irreversible reaction, the reaction rate is given by film theory as:

$$\mathcal{R} = A \frac{C_s \sqrt{KD_\ell}}{\tanh \varphi} \left[1 - \left(\frac{VK_\ell}{AD_\ell} \varphi \sinh \varphi \cosh \varphi + \cosh^2 \varphi \right)^{-1} \right]$$

(4.6)

where V is the reactor volume, K is a kinetic constant, K_ℓ the mass transfer coefficient and D_ℓ the diffusivity in the liquid phase.

If the Hatta number $\varphi = (KD_\ell)^{0.5}/K_\ell$ is greater than 2, Eq. [4.6] simplifies to:

$$\mathcal{R} = A \sqrt{KD_\ell} \, C_s$$

(4.7)

This condition is verified for the absorption of oxygen in catalyzed sodium sulfite solutions, so that this method can be used to evaluate gas liquid interfacial area.

Moreover, if an independent measurement of the interfacial area is known, as that of non cavitating vortex, an estimate of the constant KD can be made.

4.1.2.3. Emulsion stability.

The emulsion stability can be measured by degradation experiments in a vessel equipped with different stirrers at different velocities under same standard conditions.

The efficiency of a stirrer in terms of low mechanical stress on the emulsion may be characterized by observing the degradation phenomenon at constant stirrer speed.

By this method it is possible to obtain an empirical classification of the behavior of the various types of stirrers with respect to this complex phenomenon.

4.1.3. Impeller selection: laboratory experiments

A series of experiments was planned in the laboratory in order to perform a screening among some stirring devices that appeared promising on the basis of previous experience.

The experimental apparatus is a 3 1 unbaffled jacketed glass vessel as the one shown in Fig. 6, stirred by an agitator drawn by a variable speed electric motor and with interchangeable impellers.

Three different types of impellers were examined:

axial propeller;

radial curved blade impeller;

special radial impeller with modified blades.

In principle all these stirrers could produce the desired effect of high interfacial area without excessive emulsion stress.

The determination of the vortex depth yielded the results plotted in Fig. 27 as a function of revolutions per minute N and impeller type.

It is apparent from this graph that for a given stirrer speed the special radial impeller shows the highest interphase contact area in the absence of impeller cavitation.

When cavitation of the impeller is present the interphase area is the sum of the vortex area and bubble area generated in the mass of fluid.

The total area can be measured by the sulfite oxidation method using Eq. [4.7] if the parameter $\sqrt{KD}$ is known and the reaction rate is determined.

Conversely the parameter $\sqrt{KD}$ can be computed by a series of experiments of sulfite oxidation with non cavitating impeller and therefore with independently known area.
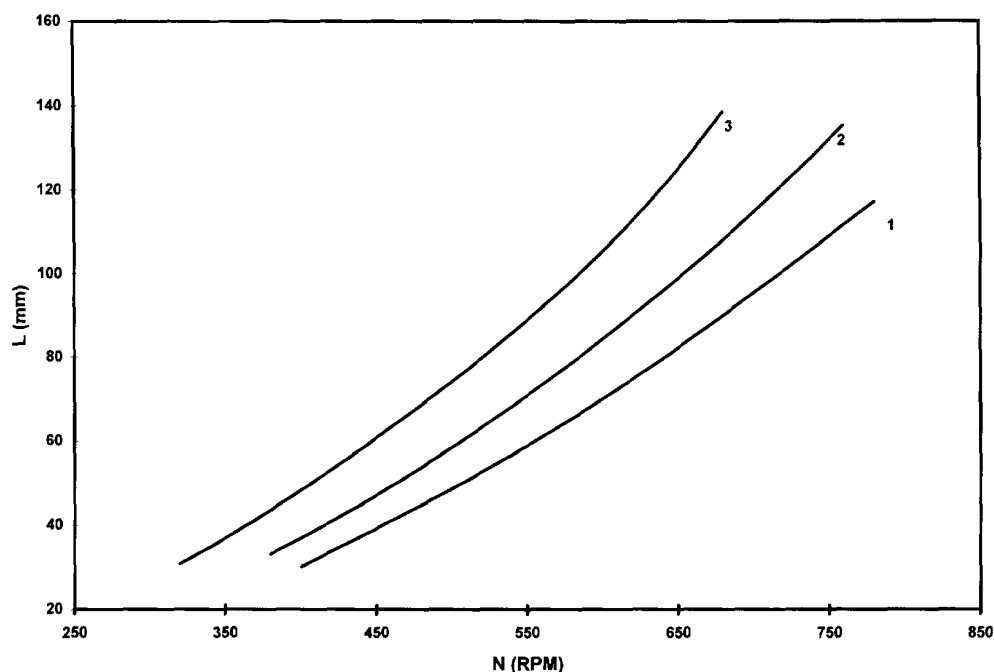

Fig. 27. Vortex depth vs. stirrer speed for the examined impeller in 3 1 cold model. 1 radial impeller; 2 axial propeller; 3 special radial impeller.
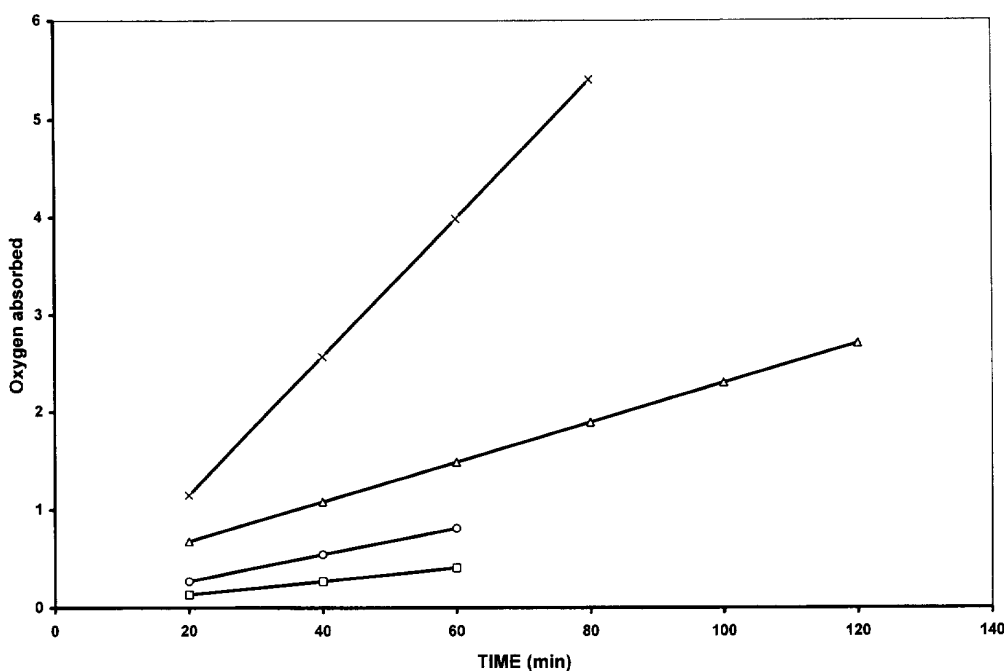
Fig. 28. Oxygen absorption in 3 l cold model-special radial impeller. (□) N = 570; (○) N = 660; (△) N = 720; (×) N = 820.

Great care must be taken when using the sulfite method.

As a matter of fact a strict control of the operating conditions such as impurities, quantity of catalyst, temperature, pressure and sulfite concentration is necessary in order to obtain valuable experimental data.

The best results were obtained using distilled water, avoiding any contacts of the solution with metallic surfaces and operating the kinetic experiments at 35°C and 1 bar oxygen pressure with 160 mg/l copper catalyst and 40 g/l sulfite concentration.

Under these conditions the reaction is independent of sulfite concentration and consequently the kinetic curves are straight lines (Fig. 28).

As shown in these figures, for every agitator, the slope of the lines and consequently the reaction rate and the interphase surface increases with stirrer speed.

This effect is better seen in Fig. 29 where for the three stirrers used, the interphase area is plotted vs. the stirrer speed. The graph shows the huge increase in surface when cavitation occurs and clearly indicates the special radial impeller as the one producing the higher interphase contact area.

Other experiments were made in order to find out the optimum impeller position but they gave less significant results.

Degradation experiments with emulsions produced in the pilot reactor were performed to obtain data on the behavior of the examined impellers. These data and those obtained by oxidation experiments were used for impeller selection.

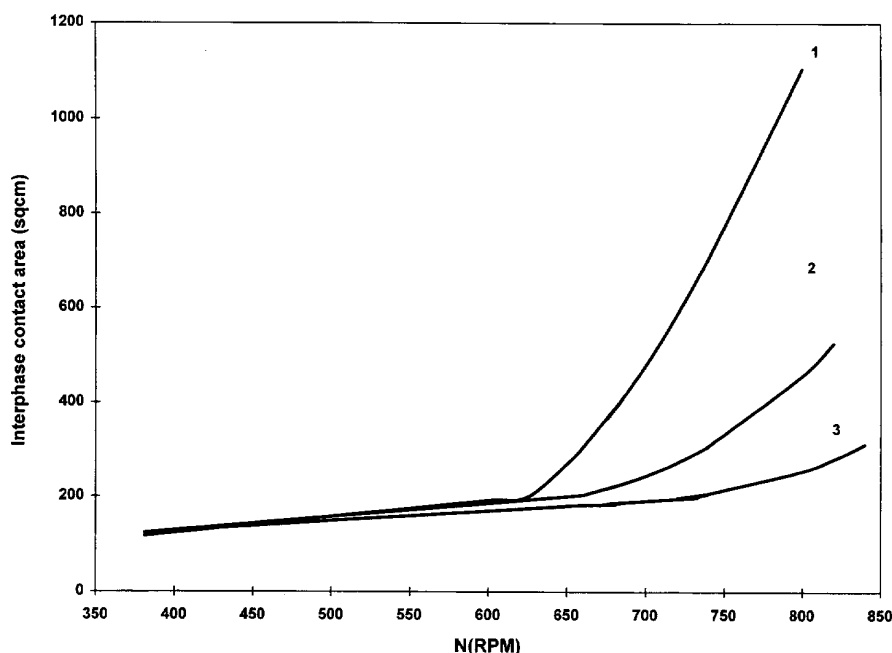The special radial impeller was chosen.

Fig. 29. Sulfite method-interphase contact area vs. stirrer speed for various impellers in 3 l cold model. 1 special radial impeller; 2 axial propeller, 3 radial impeller.

4.1.4. Scale-up procedures: experiments at the pilot scale

A rule has to be defined for the conservation of the specific interphase area in the scale-up from the laboratory to the pilot and finally to the industrial reactor. For an impeller speed N less than a critical value N_c, that is under non cavitating conditions, this area is given by Eq. (5), so that the scale-up rule is straightforward.

When cavitation occurs $(N > N_c)$ the interphase area per unit volume of the reactor is given by:

$$a = a_C + a_B \tag{4.8}$$

where a_C = area of the vortex/volume of the reactor, a_B = area of bubbles/volume of the reactor, so that Eq. (4.5) does not hold any longer.

Experiments were performed, both in the laboratory 3 l reactor and in a 50 l glass vessel, full scale with the pilot reactor, in order to determine how the vortex shape is modified by cavitation. Visual observation showed that while the lower part of the vortex, which interacts with the impeller, is no more detectable, the upper part of it still maintains a shape similar to that under non cavitating conditions (Fig. 30).

Moreover it was experimentally found that the height L_f of the vortex at the vessel wall for $N > N_c$ still obeys Eq. (4.4), as when cavitation is absent (Fig. 32).

This suggests that the vortex shape, under cavitating conditions, can still be represented by Eq. (4.2) for $r > \bar{r}$, if $\bar{r}$ (Fig. 30) is the radius where the vortex comes in contact with the impeller.

So the vortex area, that determines a_C in Eq. [4.8], can be computed by an equation similar to (4.5). Actually it does not make a great difference if one assumes that a_C is given by Eq. [4.5] evaluated at $N = N_c$, since this is a good approximation for N not much greater than N_c, while, for
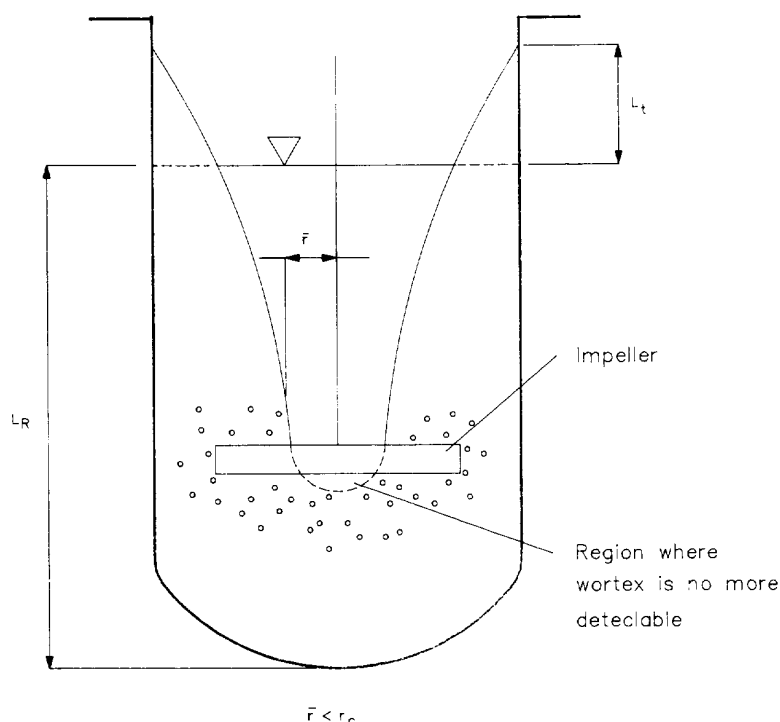
Fig. 30. Cavitating vortex schematization.

higher speeds, a_C becomes negligible compared to a_B, and therefore its exact value is not essential for scale-up purposes.

Thus, in order to scale-up a_C, only a rule for scaling the parameter r_C/r_R is needed.

Nagata [39] has shown that this parameter is a function of the Reynolds number:

$$\frac{r_c}{r_R} = \frac{d_\ell}{d_R}\left(\frac{R_e}{\alpha + \beta Re}\right) \tag{4.9}$$

The experimental data for L_l (Fig. 31) can be used to determine the constants α and β for the selected impeller, using Eq. (4.4) to correlate them.

Once the scale-up rule for r_C/r_R is known, the critical stirrer speed N_c also can be computed for different reactor scales, using Eq. [4.3] and setting L_v equal to the depth of the impeller. Using these computed values for r_C/r_R and N_c, the evaluation of a_c from Eq. [4.5] is straightforward.In order to evaluate a_B, one can write:

$$a_B = \frac{6\varepsilon_g}{d_{32}} \tag{4.10}$$

where ε_g is the gas hold-up and d_{32} is the Sauter mean diameter of bubbles.

Without cavitation   With cavitation

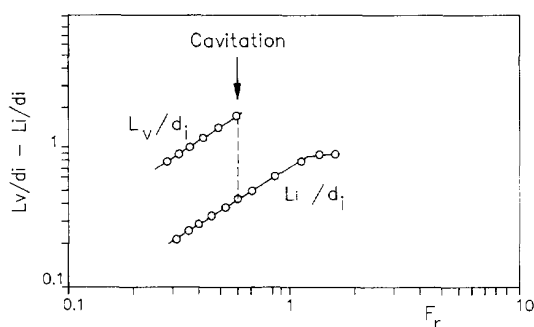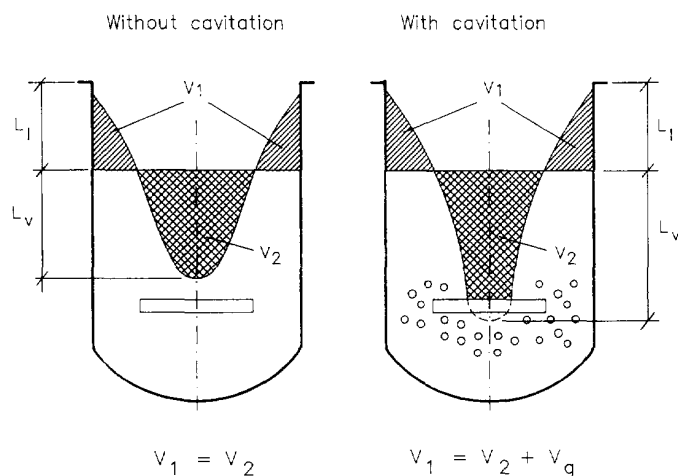$$V_1 = V_2 \qquad\qquad V_1 = V_2 + V_g$$

Fig. 31. Gas volume evaluation.

According to Hinze [32] d_{32} can be related to the Weber number:

$$\frac{d_{32}}{d_I} = \gamma\, We^{-3/5} \tag{4.11}$$

where γ is a constant dependent on reactor shape and on impeller type of diameter d_I and:

$$We = \frac{\rho\,(N/60)^2\,d_I^3}{\sigma} \tag{4.12}$$

The gas hold-up ε_g is by definition the ratio between the volume of gas and the volume of the liquid. The volume of gas, under cavitation conditions, may be assumed equal to the dotted volume in Fig. 30. As a matter of fact, since it was assumed the upper part of the vortex has the same profile it has when there is no cavitation, some gas volume must be entrained in the liquid, when the lower part of the vortex disappears, in order to maintain the same law (Eq. 4.4) for the liquid height L_l.
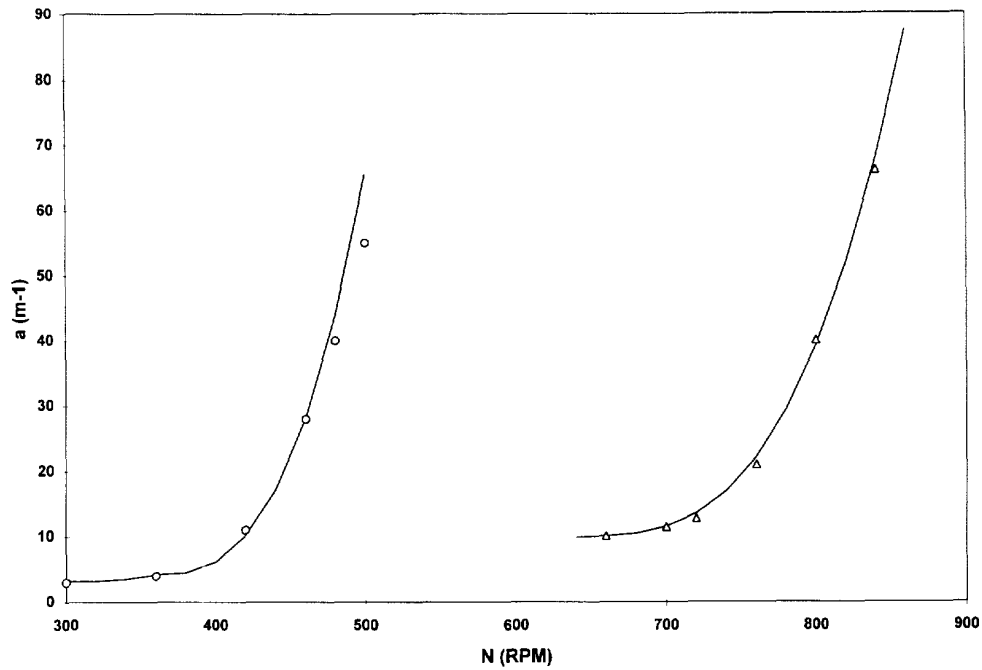
Fig. 32. Interphase contact area vs. stirrer speed in 3 l (△) and 50 l (○) models. Comparison between theory and experiments.

Under this assumption, the gas volume V_g can be computed using Eq. [4.2] as:

$$V_g = 2\pi r_c^4 \frac{\omega^2 - \omega_c^2}{2g} \left[1 - \left(\frac{\omega_c}{\omega} \right)^2 \right] \left\{ 1 - \left(\frac{r_c}{r_R} \right)^2 \left[\frac{3}{4} + \ln\left(\frac{r_R}{r_c} \right) \right] \right\}^2$$ (4.13)

Eq. [4.13] holds until (see Fig. 30): $\bar{r} < r_c$ where

$$\frac{\bar{r}}{r_c} = \left[1 - \left(\frac{\omega_c}{\omega} \right) \right] \left\{ 2 - \left(\frac{r_c}{r_R} \right)^2 \left[\frac{3}{2} - 2\ln\left(\frac{r_R}{r_c} \right) \right] \right\}^{1/2}$$ (4.14)

that is for N not too much larger than N_c. Using Eq. (4.10) to (4.13) one can write:

$$a_B = \gamma \frac{\rho^{3/5}(N/60)^{16/5} d_t^{9/5}}{2g\sigma^{3/5}} \left(\frac{d_t}{L_R} \right) \left[1 - \left(\frac{N_c}{N} \right)^2 \right]^2 \left(\frac{r_c}{r_R} \right)^4 \left\{ 1 - \left(\frac{r_c}{r_R} \right)^2 \left[\frac{3}{4} + \ln\left(\frac{r_R}{r_c} \right) \right] \right\}^2$$ (4.15)

If geometrical similarity is maintained and the same fluids (gas and liquid) are used, and assuming that a_C is negligible compared to a_B and that r_C/r_R is approximately constant, the scale-up rule based on constant interfacial area per unit volume simplifies to:

$$N^{3.2} d_t^{1.8} \left[1 - \left(\frac{N_c}{N} \right)^2 \right]^2 = \text{constant}$$ (4.16)

Assuming N_c/N does not vary too much in the scale-up, Eq. (4.16) can be further simplified to:

$$N d_t^{0.56} = \text{constant}$$ (4.17)

Actually Eq. [4.17] can be used to obtain a first guess for N, and Eq. [4.16] employed to refine the estimate. A final check can be made using the more rigorous Eq. [4.8], when necessary.

The interfacial area per unit reactor volume was experimentally determined by sulfite oxidation, both in the 3 l and in the 50 l reactor.

Results are plotted in Fig. 32, where continuous lines were drawn computing a_B and a_C as described in this section.

4.1.5. Studies in pilot polymerization reactors

As already stated, for a fast first order reaction the overall rate depends on the interphase contact area.

If this is still true for a very complex reaction set such as the radical polymerization under study, the monomer demand per unit time and unit volume must have the same dependence on the stirrer speed, as the oxygen absorption (per unit time and unit volume) in sulfite oxidation. In order to verify this assumption, parallel experiments were performed in the polymerization pilot 50 l. autoclave and in the 50 l. sulfite oxidation reactor. The stirring device was the one currently used in the pilot, that is the axial propeller.

The experimental results are shown in Fig. 33 where the monomer demand and the interphase contact area vs. stirrer revolutions per minute are plotted.

As it can be seen, choosing a proper scale for the monomer demand and the interphase contact area, the experimental points lie on the same curve. This shows that the interphase contact area is an important parameter to be used in scale-up procedures. Obviously the emulsion stability must be conserved in the scale-up.
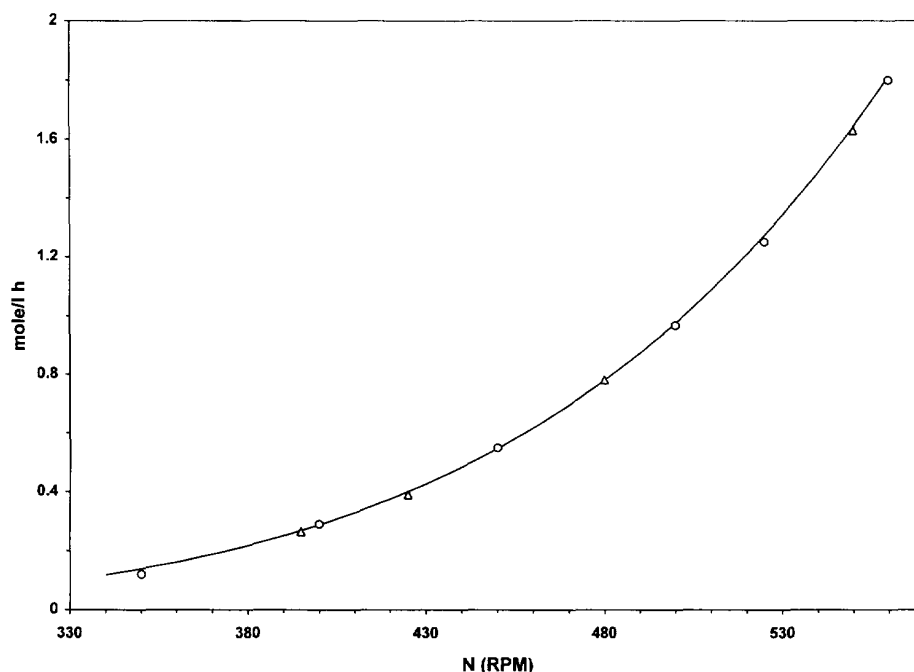

Fig. 33. Comparison between polymerization rate in 50 l. pilot reactor and interphase contact area in 50 l: cold model reactor._ interphase contact area;_ polymerization rate.

The impeller selected on the basis of cold model experiments was tried on different scales. The reaction rates agreed with those predicted by the scale-up procedure. The emulsion stability was as expected; in fact a total absence of clots in the emulsion was observed and the surfaces of the reactors at the end of the polymerization were very clean and free from any coagulated material.

4.1.6. Industrial application

The scale up rules developed have been used for the design of the stirring system of the industrial 500 l. unit and for defining optimal operating conditions.

The first result obtained was a 30% increase in productivity and 30% increase in latex concentration that is producing 30% more polymer in the same batch time.

The experience gained on mock-up and the scale up procedure developed suggested the possibility to investigate alternative production technologies.

Latex stability studies and interphase area measurements have been made on baffled reactors.

The result was an increase of 300% of productivity and late concentration. An additional result was the design and realization of a 3 m³ reactor that alone is able to almost double the capacity of the whole industrial plant.

5. Reaction and separation technologies

5.1.1.1. Distillation with chemical reaction.
Distillation with reaction is an industrial practice when reactions must be promoted by the contemporary steady-state separation of one or more products, in order to enhance productivity.

"Rigorous" modeling of reaction plus separation continuous systems is recognized to be a quite more complicated problem than ordinary distillation calculations.

Recent literature is mainly related to the reaction of acetic acid with ethanol to yield ethyl acetate and water. Some papers deal with the propylene oxide synthesis from chlorohydrins and others, mostly devoted to the reaction technique rather than to the chemical problem, refer to a bimolecular reversible reaction.

The most popular application of this technology is the MTBE synthesis from isobutylene and methanol.

In the sequel, an industrial example will be reported for a transesterification reaction.

5.2. Reaction thermodynamics and physicochemical properties

This is a very particular example where vapor liquid equilibrium are used in order to promote reaction conversion to an economical extent.

The reaction $A + B \leftrightarrow C + D$, taking place in the liquid phase, is slightly endothermic and dramatically influenced by the thermodynamic equilibrium: the value of the equilibrium constant is of the order of 10^{-3} at the maximum allowable system temperature T_{max} as shown in Fig. 34.

The reaction is activated by a homogeneous, non volatile catalyst diluted in a 5–10% of an inert solvent (I).

The behavior of the kinetic constant with temperature, for a definite liquid phase concentration of catalyst, is shown in Fig. 34.

The volatility values of all the components (relative to B) are plotted in Fig. 35 as a function of temperature.
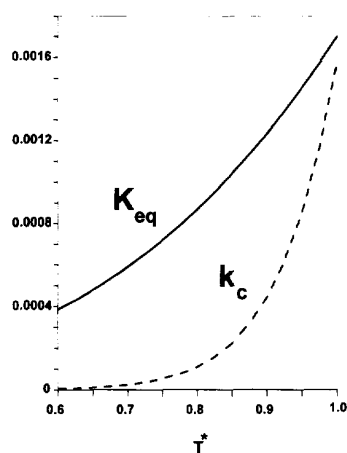
Fig. 34. Equilibrium and kinetic constant.

A is considered the light reactant, B the heavy one, C the light product and D the heavy one.

Vapor–liquid equilibrium correlation were obtained from laboratory measurements, reaction kinetics and equilibrium from liquid phase batch reaction investigations at the laboratory scale.

5.3. The reaction system

The aim of using a distillation column is to influence the equilibrium by reaching very low level of light product C, thus increasing product D concentration.

This can be achieved by stripping product C with light reactant A in the bottom of the column.

Reaction trays have a much higher hold-up than traditional separation columns, to accomplish the desired liquid residence time for reaction kinetics.

The investigated industrial system is depicted in Fig. 36.

The chemical reaction takes place only on the trays below the feed of reagents A and B, that contains the non-volatile catalyst.
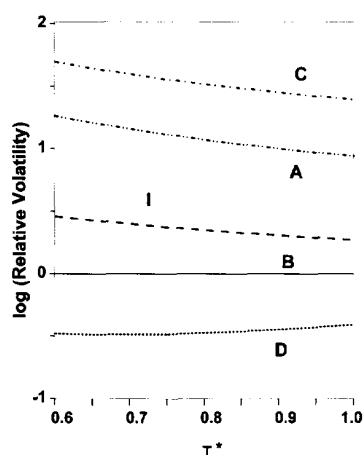

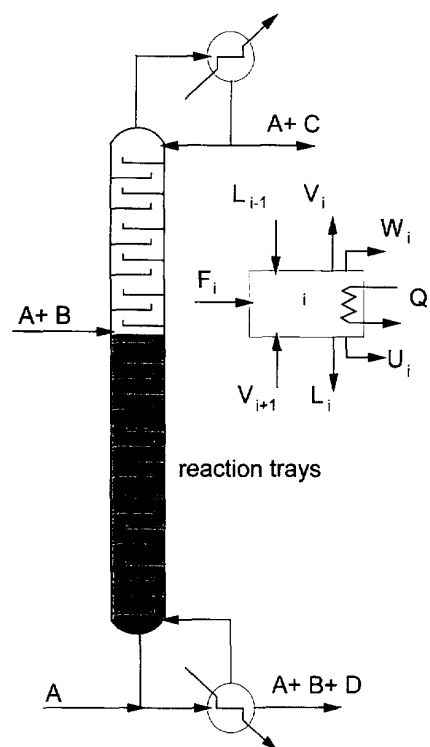Fig. 35. Volatility (B reference) dependence on temperature.

Fig. 36. Scheme of the reactive distillation column.

The upper portion of the distillation column is intended for recovering the heavy reagent B, leaving in the distillate a mixture of only A and C, that are separated in another column to recover product C and A for recycle.

5.4. Mathematical modeling and optimization

Mathematical modeling of distillation with reactions is based on the solution of the overall system of algebraic equations for all column trays.

The set of equation for tray i is a follows:

Material balance on component ($j = 1..NC$)

$$l_{j,i-1} + v_{j,i+1} - l_{j,i} + v_{j,i} + f_{j,i} - u_{j,i} - w_{j,i} + \Sigma_r \, v_{j,r} \, \lambda_{r,i} = 0$$

Table 5
Conversion (%) of reactant B as a function of the number of reactive trays

No. of reactive trays	a $VLr = 3$ (ch.eq.)	b $VLr = 3$ (ch.kin.)	c $VLr = 3$ (diffus.)
5	25.96	22.01	17.61
10	27.27	24.59	21.1
15	27.56	25.61	22.81

Enthalpy Balance

$$L_{i-1}h_{i-1}^L + V_{i+1}h_{i-1}^L - (L_i + U_i)h_i^L - (V_i + W_i)h_i^v - F_i h_i^F + Q_i = 0$$

Phase equilibrium ($j = 1..NC$)

$$y_{j,i} - K_{j,i}x_{j,i} = 0$$

Chemical equilibrium ($r = 1..NR$)

$$\prod_{j=1}^{NC} x_{j,i}^{v_{r,j}} \rho_L^{\Sigma_r v_{r,j}} - K_{r,i}^{eq} = 0$$

or Chemical kinetics ($r = 1..NR$)

$$\lambda_{r,i} - k_{r,i}^c \prod_{j=1}^{NCr} x_{j,i}^{v_{r,j}} \rho_i^{\sum_{j=1}^{NCr} v_{r,i}} \cdot \left[1 - \frac{1}{K_{r,i}^{eq}} \prod_{j=1}^{NC} x_{j,i}^{v_{r,j}} \rho_i^{\sum_{j=1}^{NC} v_{r,i}} \right] \cdot V_i^P = 0$$

For non reactive trays, the trivial equation $\lambda_{r,i} = 0$ is used.

The total number of equations is $(2\ NC + 1 + NR)\ NP$ and equals the number of variables $l_{j,i}$, $v_{j,i}$, T_i, r,i that is all the other parameters of the system, such as tray pressures, tray feeds compositions and temperatures, and tray mass and heat withdrawals – not included tray No 1 (condenser) and No NP (reboiler) – must be assigned.

Usually the condenser and reboiler heat balance equations are substituted by two compatible constraint equations to be chosen among total distillate flow rate, reflux rate or ratio, and reboiler or condenser temperature.

In the case of total condenser, the NC equations of vapor–liquid equilibrium on tray No. 1 are replaced by $NC - 1$ equations of equality of concentrations in the distillate and in the reflux, and one equation for assigning condenser temperature.

Comparison of model results with industrial runs, in terms of the conversion of component B, evidence the influence of mass-transfer resistance due to the very low level of C concentration reached in the bottom of the column.

This rate mechanism was accounted for and calibrated in the model, leading to the development of a very useful tool for process performances evaluation and optimization.

With reference to Table 4:

— Model A accounts only for chemical equilibrium (nor kinetics, nor mass transfer are included), giving therefore the maximum achievable conversion for a given set of operating conditions.

— Model B accounts for equilibrium influenced chemical kinetics, allowing the study of residence time effects (liquid hold-up):

— Model C takes into account both kinetics and light product mass transfer resistance, giving conversion values close to the experimental one.

Tables 5 and 6 summarize the results of a parametric analysis on the reaction/distillation

Table 6
Conversion (%) of reactant B as a function of the vapor to liquid feed molar ratio (10 reactive trays)

V/L feed molar	a (ch.eq.)	c (diffus.)
1	19.95	17.18
3	27.27	21.10
5	36.60	27.04

performances of the number of reaction trays (global liquid hold-up) and the vapor to liquid feed ratio (stripping effect). It can be seen that, with respect to usual industrial conditions, (10 trays, $VLr = 3$) there is room for further optimization.

References

[1] R. Aris, The Mathematical theory of Diffusion on Reaction in Permeable Catalysis, Vols. I and II, Oxford University Press, London.

[2] G. Astarita, Mass Transfer with chemical Reaction Elsevier, Amsterdam, 1967.

[3] G.S.G. Beveridge and R.S. Schechter, Optimization: Theory and Practice, McGraw-Hill, New York, 1970.

[4] G. Biardi, G. Donati, A. Cotrone and G. Buzzi Ferraris, Ing. Chim. Ital., 8(3) (1972) 40–47.

[5] R.B. Bird, W.E. Stewart and E.N. Lightfoot, Transport Phenomena, Wiley, New York, 1960, p. 570.

[6] G.E.P. Box, W.G. Hunter and J.S. Hunter, Statistics for Experimenters an Introduction to Design, Data Analysis and Model Building, Wiley, New York, 1978.

[7] G. Buzzi Ferraris, Ing. Chim. Ital., 4(12) (1968) 171–192.

[8] G. Buzzi Ferraris and G. Donati, Ing. Chim. Ital., 6(1) (1970) 1–11.

[9] G. Buzzi Ferraris and G. Donati, Quelques remarques sur deux modèles cinetiques de la Synthese de l'ammoniac, Colloque sur les modèles mathematiques, PAV 1970.

[10] G. Buzzi Ferraris and G. Donati, Ing. Chim. Ital., 10(7/8) (1974) 121-126.

[11] G. Buzzi Ferraris, G. Donati and F. Rejna, Automatic Building of Kinetic Models for Heterogeneous Catalysis with Integral Conversion Data European Federations of Chemical Engineering Dechema – Computer Application in Process Development, pp. 43–59, Erlangen, 1974.

[12] G. Buzzi Ferraris, G. Donati and S. Carra, Chem. Eng. Sci., 29 (1974) 1621–1627.

[13] G. Buzzi Ferraris and G. Donati, Ing. Chim. Ital., 10(6) (1974) 107–111.

[14] G. Buzzi Ferraris and G. Donati, Chem. Eng. Sci., 29 (1974) 1505–1509.

[15] P.H. Calderbank, Mixing Theory and Practice, Vol. II, Academic Press, London, 1967.

[16] P.V. Danckwerts, Gas–Liquid Reactions, McGraw-Hill, New York, 1970.

[17] J. F. Davidson and D. Harrison, Fluidized Particles, Cambridge University Press, Cambridge, 1963.

[18] M. Dente, A. Cappelli and A. Collina, Ing. Chim. Ital., 3(7/8) (1967) 137–142.

[19] M. Dente, G. Biardi and E. Ranzi, ISCRE 2 Proceedings, Chem. Eng. Sci., 22 (1972) B5–13.

[20] G. Donati and G. Buzzi Ferraris, Ing. Chim. Ital., 8(7/8) (1972) 183–192.

[21] G. Donati, L. Marini and G. Marziano, Chem. Eng. Sci., 37(8) (1982) 1265–1282.

[22] G. Donati, R. Paludetto and E. Rossi, Material and Energy Balances of Large Chemical Processes, 8th International Symposium Large Chemical Plants, Antwerp 12–14 October 1992, Proceedings, pp. 95–101.

[23] H.R. Draper and H. Smith, Applied Regression Analysis, Wiley, New York, 1966.

[24] D.C. Dyson and J.M. Simon, Ind. Eng. Chem. Fundam., 7(4) (1968) 605.

[25] Flow Sheet Simulation for the Process Industries, AspenTech.

[26] C. Freyer and O.E. Potter, Ind. Eng. Chem. Fundam., 11(3) (1972).

[27] G.F. Froment and K.B. Bischoff, Chemical Reactor Analysis and Design, Wiley, New York, 1979.

[28] E.M. Fuller, P.D. Schettler and J.C. Giddings, Ind. Eng. Chem., 58(5) (1966) 19.

[29] E.J. Henley and E.M. Rosen, Material and Energy Balance Computations, Wiley, New York, 1969.

[30] R. Hooke and T.A. Jeeves, J. Assoc. Computing Machinery 8 (1961) 212.

[31] O.A. Hougen, K.M. Watson and R.A. Ragatz, Chemical Process Principles, Vols. I and II, Wiley, New York, 1959.

[32] O. Hinze, Am. Chem. J., 1 (1955) 289.

[33] ISCRE 12, Chem. Eng. Sci.

[34] H. Kramers and K.R. Westerterp, Elements of Chemical Reactor Design and Operation, Netherlands Univesity Press, Amsterdam, 1963.

[35] D. Kunii and O. Levenspiel, Fluidization Engineering, Wiley, New York, 1969.

[36] M. Leva, Fluidization, McGraw-Hill, New York, 1959.

[37] S.M. Maron and D. Turnbull, Ind. Eng. Chem., 35 (1942) 544.

[38] S.M. Maron and D. Turnbull, J. Am. Chem. Soc., 64 (1942) 2195.

[39] S. Nagata, Mixing Principles and Applications, Wiley, New York, 1975.

[40] J.A. Nelder and R. Mead, Computer J., 7 (1965) 308.

[41] A. Nielsen, An Investigation on Promoted Iron Catalysts for the Synthesis of Ammonia, Gjellerup Forlag, Copenhagen, 1968.

[42] I. Pasquon and M. Dente, Chim. Ind. Gènie Chim., 101(10) (1969) 1431–1438.

[43] Perry Chemical Engineering Handbook, 6th edn., R.H. Perry and D.W. Green, McGraw-Hill, 1984.

[44] C.H. Satterfield, Mass Transfer in Heterogeneous Catalysis, MIT Press, Cambridge, MA, 1970.

[45] M.J. Sham, Ind. Eng. Chem., 59(1) (1967) 72.

[46] M.I. Temkin and V.M. Pyzhev, Zhr. Fiz. Khim., 13 (1939) 851.

[47] V.W. Uhl and J.B. Gray, Mixing Theory and Practice, Vols. 1 and 2, Academic Press, New York, 1966.

[48] C. Van Heerden, Ind. Eng. Chem., 45 (1953) 1242.

[49] K.R. Westerterp, Ph.D. Thesis, Delft University of Technology, The Netherlands, 1962.

[50] W.G. Whitman, Chem. Met. Eng., 29 (1923) 147.

[51] F.A. Zenz and D.F. Othmer, Fluidization and Fluid Particle Systems, Reinhold, New York, 1960.

[52] V. Arcella, G. Caputo, G. Donati, M. Gramondo and G. Santacasa, Ing. Chim. Ital., 18(3/4) (1982).